

ÉCOLE NATIONALE SUPÉRIEURE DES
TÉLÉCOMMUNICATIONS PARIS
DÉPARTEMENT TSI
SIGNAL - IMAGES

RHEINISCH-WESTFÄLISCHE TECHNISCHE
HOCHSCHULE AACHEN
LEHRSTUHL FÜR MESSTECHNIK
UND BILDVERARBEITUNG

DIPLOMARBEIT

CORTICAL SURFACE EXTRACTION AND SEPARATION
OF THE HEMISPHERES IN MRI DATASETS BY 3D
SEGMENTATION

ERFASSUNG DER KORTIKALEN OBERFLÄCHE UND
TRENNUNG DER HEMISPHÄREN IN
MRI-DATENSÄTZEN MITTELS 3D-SEGMENTIERUNG

Daniel Ruijters
Matr.-Nr. 195254

Prüfer:

Prof. Dr.-Ing. Dietrich Meyer-Ebrecht

Betreuer:

Prof. Dr. Isabelle Bloch
Dipl.-Inform. Thorsten Klein

Paris, den 10. Mai 2001

I hereby declare that this submission is my own work and that it was performed only making use of the indicated aids. All parts, which literally or generally have been based on published and unpublished sources, are acknowledged as such.

Hiermit versichere ich, daß ich die vorliegende Diplomarbeit selbständig und nur unter Benutzung der angegebenen Hilfsmittel angefertigt habe. Alle Stellen, die wörtlich oder sinngemäß aus veröffentlichten und nicht veröffentlichten Schriften entnommen sind, sind als solche kenntlich gemacht.

Paris, den 10. Mai 2000

(Daniel Ruijters)

Abstract

Objectives of this project are the extraction of the cortical surface and the morphological separation of both hemispheres in MRI images. These objectives serve the construction of individual models of the head. In order to achieve our goals, we do not start with the raw MRI data, but assume some anatomical parts of the brain to be already segmented. We base our approaches for a large part on mathematical morphology, because of its robustness and topology preserving possibilities.

For the cortical surface extraction one of the major constraints is that the obtained surface must have the topology of a hollow sphere. A topology that the cortical surface in reality possesses, but is not necessarily found in MRI images, because of their limited resolution. This topology is of importance when back projecting (inverse problems) signals measured on the scalp, such as MEG and EEG, to locate their sources on the cortex.

The separation of the cerebral hemispheres allows us to access both hemispheres individually. Since both hemispheres host different brain functions, this might be of interest. This gives us also much better access to the cortical surface within the fissura longitudinalis (the very narrow and deep furrow between the two hemispheres).

Kurzfassung

Die Ziele dieser Arbeit sind zum einen die Erfassung der kortikalen Oberfläche und zum anderen die Trennung der beiden Hemisphären in MRI Bilder mittels morphologischer Operationen, die sich wegen ihrer Robustheit und der Topologie erhaltende Eigenschaften besonders eignen. Die Arbeit ist ein Teil eines Projektes, in dem die Konstruktion von individuellen anatomischen Kopfmodellen erreicht werden soll.

Eine der wichtigsten Voraussetzungen, die der gesuchte kortikalen Oberfläche unterstellt wird, ist die Topologie eine Hohlkugel. Die reale kortikale Oberfläche besitzt zwar diese Topologie, aber in MRI Bilder wird diese wegen der beschränkte Auflösung nicht unbedingt gefunden. Für die Rückprojektion der Signale (z.B. beim EEG und MEG) auf die Kopfoberfläche ist diese Topologie von großer Bedeutung, um die entsprechenden Quellen zu lokalisieren.

Die beiden Hemisphäre haben jeweils spezialisierte Hirnfunktionen. Die Trennung der Hemisphären erlaubt, die Volumen der beiden Hemisphären einzeln zu betrachten. Durch die Trennung wird einen besseren Zugang zur Fissura Longitudinalis (der enge Spalt zwischen den beiden Hemisphären) ermöglicht.

Contents

1	Introduction	1
1.1	General introduction	1
1.2	The Comobio project	3
2	Basic concepts	4
2.1	MRI Images	4
2.2	Neighbourhood	4
2.2.1	Connectivity paradox	5
2.2.2	Simply connected components	6
2.2.3	Surface	6
2.3	Mathematical morphology	7
2.4	Topology and homotopic transformations	8
2.5	The Distance Transformation	8
2.6	Image segmentation	9
I	Cortical surface extraction	10
3	The cortical surface	11
3.1	Segmentation of the cortex: state of the art	11
3.2	Research question	12
3.3	Limitations and difficulties	12
4	Approach	14
4.1	Pre-segmented volumes	14
4.2	Main principle	14
5	Results	18
5.1	Experimental results	18
5.2	Discussion	18

II	Separation of the hemispheres	22
6	The hemispheres	24
6.1	Separation of the hemispheres: state of the art	24
6.2	Research question	25
6.3	Limitations and difficulties	25
7	Approach	26
7.1	Marker volumes: erosion of the cerebrum	26
7.2	Problems with marker volumes: growing into each other	27
7.2.1	Justification: rectangular markers	28
7.2.2	Justification: intersection of the markers	29
7.3	Multiple dilation	30
7.3.1	Meeting markers	30
8	Results and discussion	31
8.1	Experimental results	31
8.2	Limitations and difficulties	32
8.3	Discussion and prospects	32
9	Conclusion	39
9.1	The cortical surface	39
9.2	The hemispheres	40
A	Implementation of the algorithms	41
A.1	introduction	41
A.2	The conditional dilation	42
A.2.1	distance transform	42
A.2.2	priority waiting list system	42
A.3	Justification of the marker volumes	44
A.3.1	Creating rectangular markers	44
A.3.2	Creating intersected markers	44
A.4	The multiple dilation	45
	Bibliography	47

List of Figures

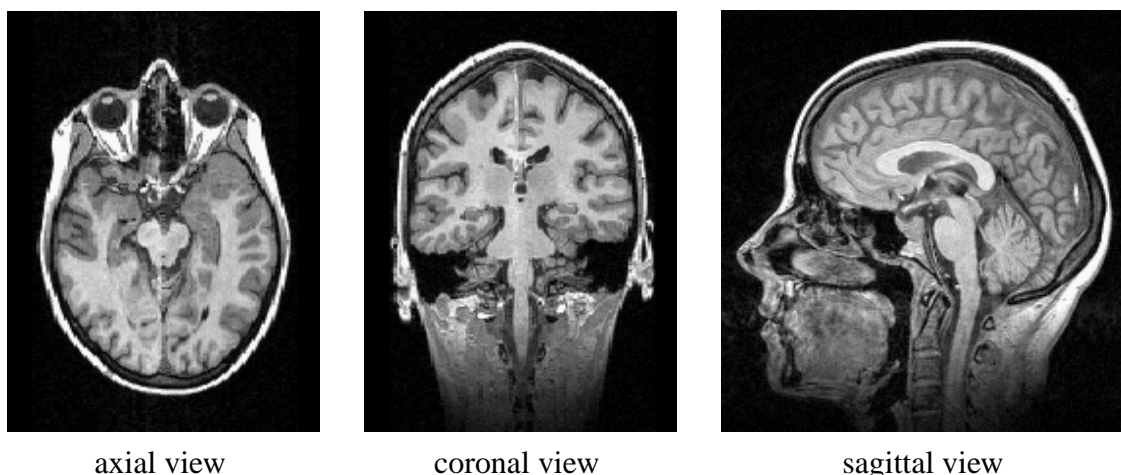
1.1	MRI scan	1
2.1	4- and 8-connectivity	5
2.2	6-, 18 and 26-connectivity	5
2.3	Connectivity paradox: (a) closed ring, (b) ambiguous ring	6
2.4	(a) Elementary cells of edge uv for 4-connectivity, (b) Two equivalent paths from p to q , and (c) two non-equivalent paths	7
2.5	Objects and their homotopic tree	8
3.1	(a) closed cavity because of partial volumes, (b) red line: real cortex surface	13
4.1	White matter and cortex	16
4.2	(a) closed cavity because of partial volumes, (b) red line: real cortex surface, (c) opened cavity	16
4.3	Flowchart of the procedure to obtain the cortical surface	17
5.1	The cortical surface, lower slides	19
5.2	The cortical surface, upper slides	20
5.3	3D representation of the cortical surface, upper front view	21
5.4	3D representation of the cortical surface, lower view	21
7.1	Flowchart of the procedure to obtain the hemispheres	27
7.2	Marker1 grows into the other hemisphere	28
7.3	Rectangular markers	29
7.4	(a) Intersection of markers in y,z (b) scanline in x -direction	29
7.5	Meeting markers: (a) stair effect, (b) zigzag effect	30
8.1	The separated hemispheres in 3D	31
8.2	Unjustified marker volumes	33
8.3	Separated hemispheres, obtained from unjustified markers	33
8.4	Example of unjustified marker volumes	34
8.5	Example of a marker that grew into the other hemisphere	34
8.6	Rectangular marker volumes	35
8.7	Separated hemispheres, obtained from rectangular markers	35
8.8	Intersected marker volumes	36

LIST OF FIGURES

8.9	Separated hemispheres, obtained from intersected markers	36
8.10	3D representation of a hemisphere (pictured under two different angles), obtained with rectangular markers	37
8.11	3D representation of a hemisphere (pictured under two different angles), obtained with intersected markers	37
8.12	Separated hemispheres, obtained from rectangular markers	38
8.13	Separated hemispheres, obtained from intersected markers	38
A.1	Distance transformation of the white matter into the cerebrum	42

Chapter 1

Introduction



axial view

coronal view

sagittal view

Figure 1.1: MRI scan

1.1 General introduction

The development of medical imaging techniques, like MRI (Magnetic Resonance Imaging), allows the three-dimensional measurement and visualization of the internal brain structures of in-vivo subjects. An anatomical representation is not necessarily an aim in itself, but can serve more objectives, like the detection of pathologies or the study of the functioning of the brain. The ability to analyse and diagnose the human brain without surgery is a great advantage and the last years have witnessed a huge evolution of brain imaging applications. A description of the technical details of the MRI scanning technique can be found in literature, e.g. [Bra89].

The vast flood of image data delivered by these techniques calls for automated processing methods, like 3D segmentation. However since the form and place of the different parts of the brain may vary substantially between subjects, a fully automated segmentation is not easy to implement. Manual segmentation may be used as a last rescue, but it has major disadvantages.

Not only is it labour intensive, it is also more difficult to reproduce results. Thus automated brain segmentation is still evolving and different approaches may be suited for different problems.

The objective of this thesis is to retrieve the surface of the cerebral cortex and to separate both cerebral hemispheres. The retrieval of volumes representing the cortex and the hemispheres will be done by using mathematical morphology. Mathematical Morphology is very often used in applications where shape of objects and speed is an issue [SHB98].

A representation of the cortical surface allows the retracing of signals, measured at the scalp. This permits the identification of energy sources on the cortex from EEG (electroencephalogram) and MEG (magnetoencephalogram) scans, which deliver a two-dimensional image of respectively the electrical field and magnetic field measured on the scalp. This procedure, referred to as “inverse problem”, can be used for identifying which parts of the cortex show high activity when performing different tasks, and thus improve our understanding of the functioning of the brain. Also it is possible to project external energy sources (such as the ones that are emitted by mobile phones) on a model of the cortical surface, and as such play a role in the research of their influence on the human brain. In this regard we also refer to [Coi99] and [Wie93].

This thesis is performed at the TSI (Signal-Images department) at the École Nationale Supérieure des Télécommunications (ENST) Paris, France, under supervision of Prof. Dr. Isabelle Bloch. It is being evaluated and supervised by the Institute for Measurement technique and Image Processing (LfM) at the University of Technology Aachen (RWTH), Germany, directed by Prof. Dr.-Ing. Dietrich Meyer-Ebrecht, and there supervised by Dipl.-Inform. Thorsten Klein. The thesis serves as part of the construction of an individual head model, based on MRI data, that is being developed at the TSI department in collaboration with the laboratory of Cognitive Neurosciences and Brain Imaging (LENA) at the Salpêtrière Hospital in Paris in order to serve the Comobio project. Since as such the thesis is not a stand-alone project, we make use of earlier results in brain segmentation done at the TSI department. The MRI images used for this thesis were provided by the LENA.

This document consists of nine chapters. In chapter 2 the foundation for the following chapters is laid. It deals with the basic mathematical and imaging theories that were applied to obtain our particular solutions for the questions that were posed for this thesis.

The chapters 3, 4 and 5 form together part I. This part tackles the cortical surface extraction, the first goal set for this thesis. In chapter 3, after a short introduction to the cortical surface, the present state of the art concerning the segmentation of the cortex is discussed briefly. Then the research question is formulated and discussed. Chapter 4 comprises the chosen approach to obtain the cortical surface. Then in chapter 5 the practical results of our approach applied to MRI images are presented.

Part II consists of the chapters 6, 7 and 8. It deals with the separation of the hemispheres, the second aim set for this thesis. After a citation of the famous lecture of Pavlov concerning the cerebral hemispheres, in chapter 6 is started with a short introduction to the hemispheres. This chapter further comprises a brief discussion of the state of the art concerning the segmentation of the hemispheres, and the formulation and discussion of the research question relating to the separation of the hemispheres. In chapter 7 the chosen approach to obtain the separation of the hemispheres can be found. In chapter 8 the results of this approach applied to MRI images are

presented and discussed.

Finally chapter 9 comprises the conclusions that were drawn from the gained results, and the prospects for future investigations. Also, a fusion between both parts is made.

1.2 The Comobio project

Along with the increasing numbers of mobile phones sold, more questions are being raised about health risks involved with their use. Providing answers demands for a comprehensive investigation to possible biological effects. The Comobio¹ project (COmmunications MOBiles et BI-Ologie) bundles resources of several French academic and industrial forces in a common effort intending to increase the knowledge of biological and sanitary effects of the microwaves emitted by mobile phones. This project merges complementary studies that can be divided in three groups: dosimetry studies, human studies, and animal studies. Participants in this project are: Alcatel, Bouygues Telecom, Cégétel, ENST Brest, ENST Paris, France Télécom, IRCOM Limoges, Sagem, Supélec, and the universities of Bordeaux, Marseille, Nîmes, Orsay and Rennes.

¹The Comobio project in the internet: see <http://www.enst.fr/comobio>.

Chapter 2

Basic concepts

2.1 MRI Images

The data obtained by the MRI scanning technique are stored in discrete three dimensional *images* in a Cartesian base: $f : \mathbb{Z}^3 \rightarrow \mathbb{N}$. Each coordinate represents a rectangular volume, called a *voxel*: $x \in \mathbb{Z}^3$. All voxels have the same dimensions. However length, width and height of a voxel are not necessarily equal. A voxel is considered to be filled with a discrete gray value representing the measured value for its coordinates. The MRI Images contain the scan of a human head, which can be segmented in several parts, such as the brain, the eyes etc. The brain itself, which is our subject of interest, can be further segmented into several volumic objects. These *objects* are represented in our MRI image by a *set of voxels*: $X \subset \mathbb{Z}^3$.

2.2 Neighbourhood

Both by human perception as well as in many operations a voxel (or a pixel for that matter) is not considered individually, but within the relationship with its local neighbourhood. The neighbourhood of a voxel is the set of its adjacent voxels. But which voxels are considered to be adjacent to a particular voxel?

Definition 2.1 *Let X be a set and $\mathcal{P}(X)$ the set of all subsets of X , then the neighbourhood is defined as $\Gamma : \mathbb{Z}^3 \rightarrow \mathcal{P}(\mathbb{Z}^3)$ [Ser82].*

In a two dimensional square grid, the \mathbb{Z}^2 space, we distinguish between two elementary neighbourhoods: the 4- and 8-connected neighbourhood (also called N_4 and N_8). In the 4-connected neighbourhood adjacent pixels share a line, thus the 4-connected neighbourhood consists of the horizontal and vertical neighbours. The 8-connected neighbourhood includes the pixels of the 4-connected neighbourhood as well as the pixels sharing a corner (point connected), the diagonal neighbours. See Figure 2.1.

In a three dimensional cubical grid, the \mathbb{Z}^3 space, we distinguish between three different elementary neighbourhoods: the 6-, 18- and 26-connected neighbourhood (N_6 , N_{18} and N_{26}).

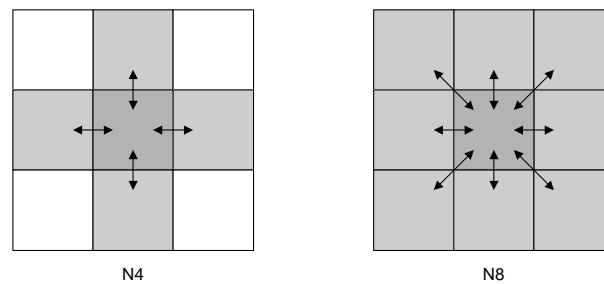


Figure 2.1: 4- and 8-connectivity

The 6-connected neighbourhood is formed by adjacent voxels sharing a face. The 18-connected neighbourhood includes these voxels as well as the ones that share a line. The 26-connected neighbourhood includes, beside the 18-connected neighbourhood, also the voxels sharing only a corner. See figure 2.2.

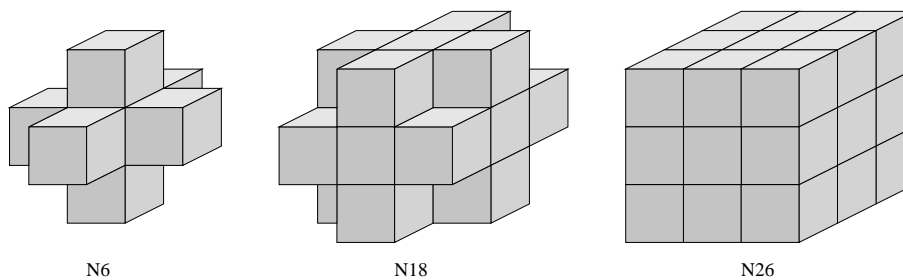


Figure 2.2: 6-, 18 and 26-connectivity

2.2.1 Connectivity paradox

Let a path $\rho_{x,y}$ be a set of points from x to y , where each point in the set is adjacent to its predecessor, according to a given discrete connectivity. An object is connected if for any two points there is at least one path within the object, which leads from one point to the other [Ros69, Ros70]. In figure 2.3a the ring of black pixels, by all reasonable definitions of connectivity, divides the image into three segments: the white pixels exterior to the ring, the black pixels of the ring itself, and the white pixels interior to the ring. The pixels within each segment are said to be connected to one another. This concept is easily understood for Figure 2.3a, but ambiguity arises when considering Figure 2.3b. Under 8-connectivity for instance, all white pixels are connected together, and all black pixels are connected as well. This paradox can be avoided by defining different connectivities for the black foreground pixels and the white background pixels [Pra91].

A similar dilemma arises in a three dimensional cubical grid. Again the solution is to choose

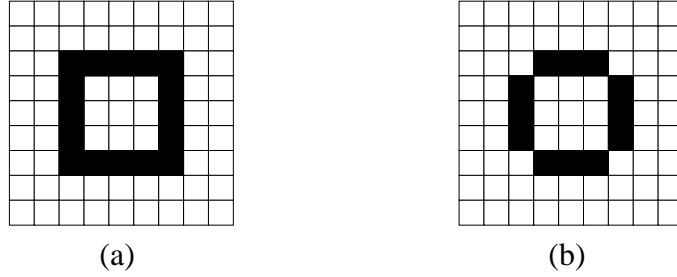


Figure 2.3: Connectivity paradox: (a) closed ring, (b) ambiguous ring

different connectivities for foreground and background. The following combinations are admissible:

- N_{18} foreground, N_6 background.
- N_6 foreground, N_{18} background.
- N_{26} foreground, N_6 background.
- N_6 foreground, N_{26} background.

We choose for our objects 26-connectivity, with consequently a 6-connected background, because 26-connectivity allows finer structures. Especially for the surface of the cortex, which is an object with a thickness of only one voxel, this is of importance.

2.2.2 Simply connected components

A loop is a path in which initial and terminal points coincide. The smallest possible loop is called an elementary cell. The elementary path joining two consecutive points u, v is *equivalent* to any other path between u and v which follows the edges of elementary cells of edge uv . Examples for the two-dimensional case can be found in figure 2.4. A set of points X is *simply connected* if there is at least one path connecting any two given points p, q within it, and if all possible paths leading from p to q are equivalent [Ser82].

This means for a 3-dimensional object that it is simply connected if it is: 1. connected, 2. it does not contain any holes (“bubbles”) and 3. it does not contain any tunnels.

Algorithm $CC_i(X)$ delivers a simply connected component in a set X , whereby $CC_1(X)$ is the largest simply connected component, $CC_2(X)$ the second largest, etc. $\#CC(X)$ denotes the number of simply connected components in X .

2.2.3 Surface

Definition 2.2 *The border of a volumic object is defined as:*

$$bd(X) = \{x \mid x \in X \wedge \Gamma(x) \cap \overline{X} \neq \emptyset\}$$

Where $\Gamma(x)$ denotes the neighbourhood of x according to a given discrete connectivity.

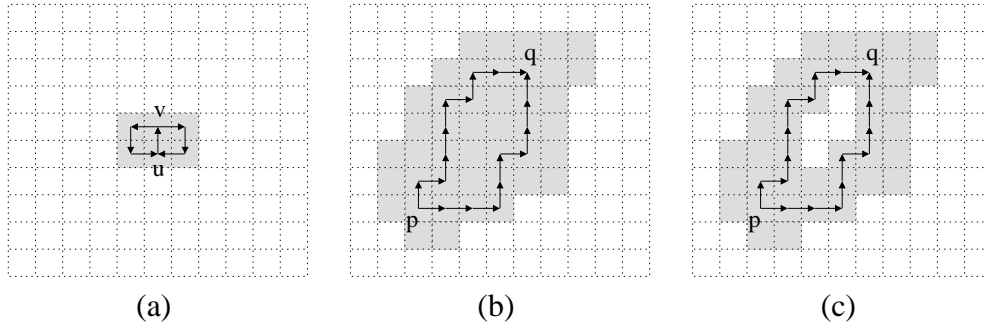


Figure 2.4: (a) Elementary cells of edge uv for 4-connectivity, (b) Two equivalent paths from p to q , and (c) two non-equivalent paths

This border delivers a “shell” of voxels corresponding to the internal surface of a volumic object. Note that the shell still consists of voxels. So even though it has a thickness of only one voxel, it still has a volume. Thus, it does not deliver a two dimensional area.

2.3 Mathematical morphology

Morphological image processing [Pra91] is a type of processing in which the spatial form and structure of objects within an image are modified. The basic concepts of morphological image processing trace back to research on spatial set algebra by Minkowski [Min03] and the studies of Matheron [Mat75] on topology and lattice theory. Serra [Ser82] developed much of the early foundation of the subject. Morphological operations, like dilation and erosion, plus many variants can be defined and implemented by “hit or miss” transformations. Mathematical Morphology is very often used in applications where shape of objects and speed is an issue [SHB98]. The basic morphological operations can be implemented in hardware, which can shorten calculation time even more [Jon92]. With the large amount of data, and thus calculations, involved in 3D operations this certainly could be taken into account.

Dilation and erosion

Dilation and erosion are two basic operations in mathematical morphology. With dilation, an object grows uniformly in spatial extent, while with erosion an object shrinks uniformly. Both operations are irreversible. For both there is a kernel B (also called structuring element) that operates on an image X . In our case image and kernel are both three dimensional discrete binary images $X, B \subset \mathbb{Z}^3$. In the discrete space the kernel generally has odd dimensions (we use symmetrical kernels of size $3 \times 3 \times 3$).

Let B_u denote the translation of kernel B by vector u . Then the dilation of an image X by a symmetrical kernel B , noted as $X \oplus B$, is the set of positions u for which B_u crosses X [SM93, SHB98]:

$$X \oplus B = \{u, B_u \cap X \neq \emptyset\} = \{x - b, x \in X \text{ and } b \in B\} \quad (2.1)$$

The erosion is the dual operation of the dilation, and can be defined using the dilation of the complement of image X . The complement of image X is denoted as X^c . The erosion of image X by a kernel B , noted as $X \ominus B$, is the set of positions u for which B_u is completely within X :

$$X \ominus B = \{X^c \oplus B\}^c = \{u, B_u \subset X\} = \{u, u - b \in X \forall b \in B\} \quad (2.2)$$

2.4 Topology and homotopic transformations

A transformation is homotopic if it does not change the contiguity relation between regions and holes in the image [SHB98], thus if it does not change the topology of an image. The contiguity relation can be expressed by the definition of connected objects (see section 2.2.1). This relation is visualized by the homotopic tree; its root corresponds to the background of the image, first level branches correspond to the objects with bounds to the background, and second level branches match holes within these objects, etc. (see figure 2.5).

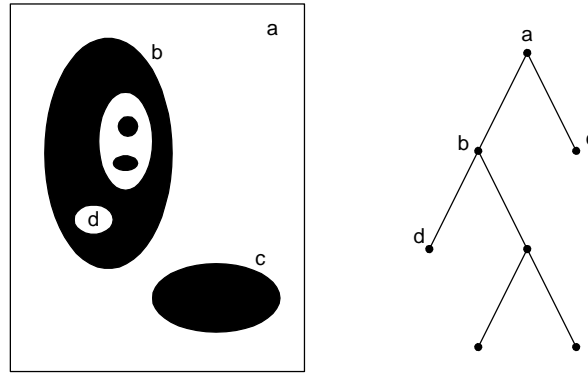


Figure 2.5: Objects and their homotopic tree

2.5 The Distance Transformation

Given three voxels $p, q, x \in \mathbb{Z}^3$, we call d a *distance function* or *metric* [GW92] if

$$\begin{aligned} d(p, q) &> 0 \forall p \neq q \\ d(p, q) &= 0 \Leftrightarrow p = q \\ d(p, q) &= d(q, p) \forall p, q \\ d(p, x) &\leq d(p, q) + d(q, x) \forall p, q, x \end{aligned} \quad (2.3)$$

The *Euclidean distance* between p and q is defined as

$$d_e(p, q) = \sqrt{(p_x - q_x)^2 + (p_y - q_y)^2 + (p_z - q_z)^2} \quad (2.4)$$

whereby (p_x, p_y, p_z) denotes the coordinates of p . However in our algorithms we use the chamfer distance [Ver91, Bor86], which is an approximation of the Euclidean distance in discrete space.

The distance between a point p and an object X is defined as

$$d(p, X) = \min\{d(p, x) \mid x \in X\} \quad (2.5)$$

The *Distance Transformation (DT)* for a point x in a set X is denoted as:

$$DT : x \rightarrow \min\{d(x, v) \mid v \in \overline{X}\} = d(x, \overline{X}) \quad (2.6)$$

v is a point in the Complement of X , thus a non-feature (background) point. Therefore $DT(x)$ is the smallest distance from x to the background of X . The result of a distance transformation can be represented as a gray level image. We can also consider the distance transformation of a point in \overline{X} .

2.6 Image segmentation

No single standard method of image segmentation has emerged [Pra91]. Rather, there are a number of methods, each of them with their own strengths and weaknesses. The term “Image segmentation” is used to describe two different kind of treatments [Coi99]. One meaning the division of image space in connected components, using only information contained in the image itself. Methods such as local feature extraction based on statistics, region growing, etc. [ME01] can serve this kind of treatment. These are low level operations, which means that they are normally applied at an early stage in the image processing pipeline.

In the other use of the term each segment represents a symbolic object. The extraction of such objects from an image requires a priori knowledge about the represented subject. In this regard the term denotes rather a whole process. In this thesis we will use the term “image segmentation” in the latter sense.

Part I

Cortical surface extraction

Chapter 3

The cortical surface

The surface layer of the cerebral hemispheres - the neocortex, or cerebral cortex - is about two millimetres thick and has a total surface area of about 1.5 square-metres. In humans, the cerebral cortex, is deeply convoluted (furrowed). The convolutions have the effect of increasing the amount of cerebral cortex without increasing the overall volume of the brain [Pin90]. The cerebral cortex is divided into four sections, called “lobes”: the frontal lobe, parietal lobe, occipital lobe, and temporal lobe. Since the neocortex plays an important role in the human cognitive processes, the importance of being able to segment and model the cortex from a MRI image may be evident.

3.1 Segmentation of the cortex: state of the art

The first step when segmenting the brain from MRI images is often the determination of the set of voxels that form the brain (the brain mask), and identifying the brain tissues, such as grey matter, white matter and cerebrospinal fluid (CSF). In many studies in a further step the discrimination is made between the large brain structures such as the cerebrum, the cerebellum and the brainstem. Though this is not sufficient to determine the cortical ribbon, the outline of the cerebrum corresponds for a large part to the exterior of the cortical folds, and thus might form a starting point in segmenting the cortex [Coi99].

Region growing Wagner *et al.* [WFW⁺95] segment the volume of the cortex making use of region growing. Depending on the growth, the voxels separate at the interface of the cortex and the white matter (grey-white interface) or at the interface of the cortex and the cerebrospinal fluid (grey-CSF interface), thus at the interior or the exterior interface. This method does not guarantee any topology, nor does it take the partial volume problem (see section 3.3) into account.

Deformable models Zeng *et al.* [ZSSD98] have proposed a method based on deformable models using *level sets*. The model is based on two parallel evolving curves under constraints of proximity. These two curves represent the grey-white and grey-CSF interfaces. The model does

3.2. RESEARCH QUESTION

not have any constraints in respect to topology. Also, it does not take the partial volume problem into account.

In [XPP⁺98], Xu *et al.* describe a fuzzy segmentation of the grey matter, the white matter and the CSF. The white matter is subsequently filtered in order to obtain an isosurface. This isosurface serves to initialize a deformable model, whereby it is pushed against the border of cortical ribbon. The use of an isosurface does not guarantee the topology of a hollow sphere. Hence the authors chose to calculate the Euler characteristics, and then to apply a median filter and to recalculate the isosurface until the desired topology is reached.

Homotopic transformations Mangin *et al.* [MCF98] use homotopic transformations to segment the cortex. As initial model they use the voxels corresponding to the tissues of the brain. They create a bounding box around the brain, and subtract iteratively simple points, imposing the topology of a hollow sphere.

Teo *et al.* [TSW97] propose a homotopic transformation using region growing. First the white matter and the CSF are segmented. Then layers of voxels are added to the white matter in order to obtain the cortex. Adding the different layers is controlled by the topology of the cortical ribbon, as a result of a redefinition of the adjacency between the voxels of the cortex. This method assures the correct topology if the segmentation of the white matter delivers a simply connected object.

3.2 Research question

Our aim is to obtain a volume corresponding to the cortical surface. One condition we impose on this surface is that it has to have the topology of a hollow sphere. This corresponds to the topology of the surface of a simply connected component. This is of importance in order to back-project signals measured on the scalp, such as EEG and MEG, or to project environmental signals on the cortex, such as electro-magnetic fields emitted by mobile phones, in order to investigate their influence on the brain. It should be noted that the real cortical surface, as we find in the human brain, in fact has the topology of a hollow sphere. Yet in MRI Images, due to discretisation, this topology may be compromised. A further goal is particularly the obtaining of the cavities in the structure of the cortex, which are filled with the cerebrospinal fluid, without compromising the topology of the surface.

We will extract the cortical surface using mathematical morphology. The choice to give mathematical morphology a major role in our particular solutions was made because of its robustness and topology preserving possibilities. Mathematical Morphology is very often used in applications where shape of objects and speed is an issue [SHB98].

3.3 Limitations and difficulties

Several features of either the brain anatomy, the MRI technique, or the combination of both may impose hurdles that have to be taken, or at least considered. First of all we should take

3.3. LIMITATIONS AND DIFFICULTIES

into consideration that the human anatomy may vary substantially between different individuals. Therefore a method should be robust in regard to inter-individual differences, and should be tried on a range of test subjects.

Pathologies may have a considerable effect on the brain morphology. If a method of brain segmentation is to be used in diagnostic medicine then it is important that it is robust against the effects of various pathologies.

The resolution of MRI images plays an important role in the segmentation of the cortex and the extraction of its surface [Coi99]. This resolution, which is in the case of MRI images currently in the order of one cubic millimetre, determines the minimal measures of the brain structures that will appear in the image. If there are several tissues to be found in the volume of one voxel, the mean value of those tissues will be represented in the image. This phenomenon, called “partial volume” tends to blur the borders between tissues.

The cavities and convolutions are particular sensible for this effect, especially when the space between two gyri gets very small. Because of this effect the gyri sometimes seem to grow together, where in reality that is not the case. As a consequence the topology of the surface, found in such a MRI scan, might be compromised. We will try to solve this in our approach.



Figure 3.1: (a) closed cavity because of partial volumes, (b) red line: real cortex surface

Chapter 4

Approach

4.1 Pre-segmented volumes

In order to extract the cortical surface, we do not start with the raw MRI image, but we assume some objects to be already segmented [DUB01]. We can make this assumption, because this thesis is done as part of a larger project (see section 1.1), and therefore we are able to build on previous results in segmenting the brain.

The white matter plays a central role in our approach, and is denoted by a set of voxels X_{white_matter} . We need our white matter to be simply connected, and therefore we define our white matter as the largest simply connected object taken from the white matter, that we receive as input:

$$X_{white_matter} = CC_1(X_{white_matter}^{input}) \quad (4.1)$$

It should be noted that the real white matter, as it is found in the brain, is in fact simply connected. This operation normally can be performed on the segmented white matter, without a lot of problems. Apart from some disconnected voxels at the edge, the resulting object will be almost the same as the input white matter.

Further we need objects representing the brain mask, the cerebellum, the brainstem and the cerebrospinal fluid (CSF). The brain mask is an object used to extract the brain from the raw MRI image, and is normally obtained as the first step when segmenting MRI brain scans.

4.2 Main principle

One of the first objects we create is a volume representing the cerebrum. We do this by subtracting the cerebellum, the brainstem and the cerebrospinal fluid from the brain mask:

$$\begin{aligned} X_{cerebrum} &= X_{brainmask} \setminus X_{cerebellum} \setminus X_{brainstem} \setminus X_{CSF} \\ &= X_{brainmask} \cap \overline{X_{cerebellum}} \cap \overline{X_{brainstem}} \cap \overline{X_{CSF}} \end{aligned} \quad (4.2)$$

Very important for recognizing correctly the cavities, convolutions and folds of the cortex, is that the cerebrospinal fluid (CSF) is not contained in the cerebrum.

4.2. MAIN PRINCIPLE

The easiest method to obtain the cortical surface would seem to simply extract the border of the volume representing the cerebrum $bd(X_{cerebrum})$. However this method does not necessarily deliver the searched topology, because it does not address the partial volume problem (see section 3.2).

Therefore we take a different approach. We start with the simply connected component corresponding to the white matter, and dilate this object, with the condition that a voxel is only added if it is part of $X_{cerebrum}$ (geodesic dilation into $X_{cerebrum}$), and if the resulting object is still simply connected. Thus, only simple points lying with the cerebrum are allowed to be added. This means that when the dilation reaches the border of the object representing the cerebrum, all voxels in $X_{cerebrum}$ are either added, or do not meet the conditions earlier mentioned. Finally from the object gained by this operation the border is taken. The flowchart of this procedure can be found in figure 4.3.

Definition 4.1 *A voxel x is a simple point if:*

$$\#CC_{26} [X \cap N_{26}^*(x), x] = 1$$

$$\#CC_6 [\bar{X} \cap N_{18}^*(x), x] = 1$$

Whereby $\#CC_n$ denotes the number of connected components according to n -connectivity, and $N_n^(x)$ the neighbourhood of x , according to n -connectivity, excluding x itself. Thus if the foreground voxels in the N_{26}^* neighbourhood of a given voxel are simply connected, according to 26-connectivity, and the background voxels in the N_{18}^* neighbourhood, including the voxel x itself, are simply connected, it is a simple point. Adding such a simple point to a simply connected component always results in an object that is again simply connected.*

Since the cortex is mainly a layer on the white matter, starting with the white matter makes sense, because it already follows the form of the cortex (see figure 4.1). The conditional dilation delivers an object that is simply connected, and therefore its surface has the right topology, the topology of a hollow sphere. In general this surface will resemble closely the surface found by $bd(X_{cerebrum})$, however especially the partial volumes, that close cavities, will not be contained in the corresponding object. And thus the cortical folds, which are unconnected in reality, but connected in the MRI image due to its resolution (see section 3.2), will be unconnected again. Parallel with this phenomenon the cavities, which were closed because of the partial volume problem, will be opened again (see figure 4.2). Hence the topology of the retrieved surface will correspond better with the topology of the real cortical surface. However it should be noted that in the case of the partial volumes it may be shifted in the order of one voxel size.

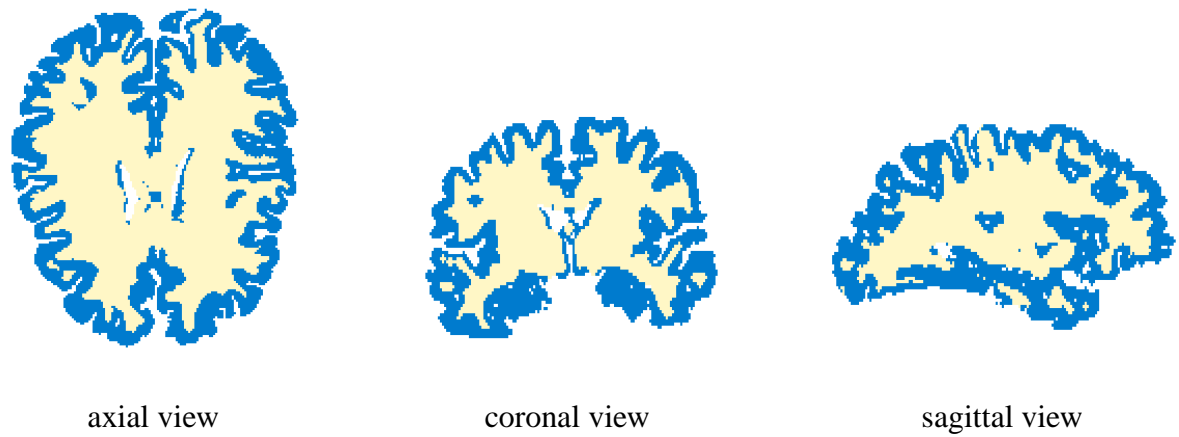


Figure 4.1: White matter and cortex

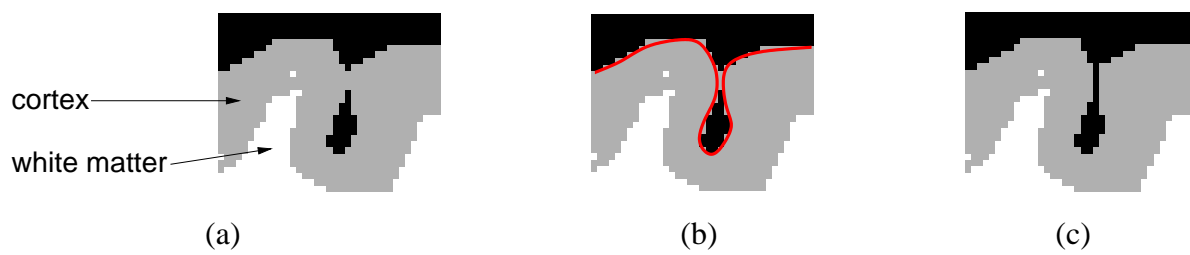


Figure 4.2: (a) closed cavity because of partial volumes, (b) red line: real cortex surface, (c) opened cavity

4.2. MAIN PRINCIPLE

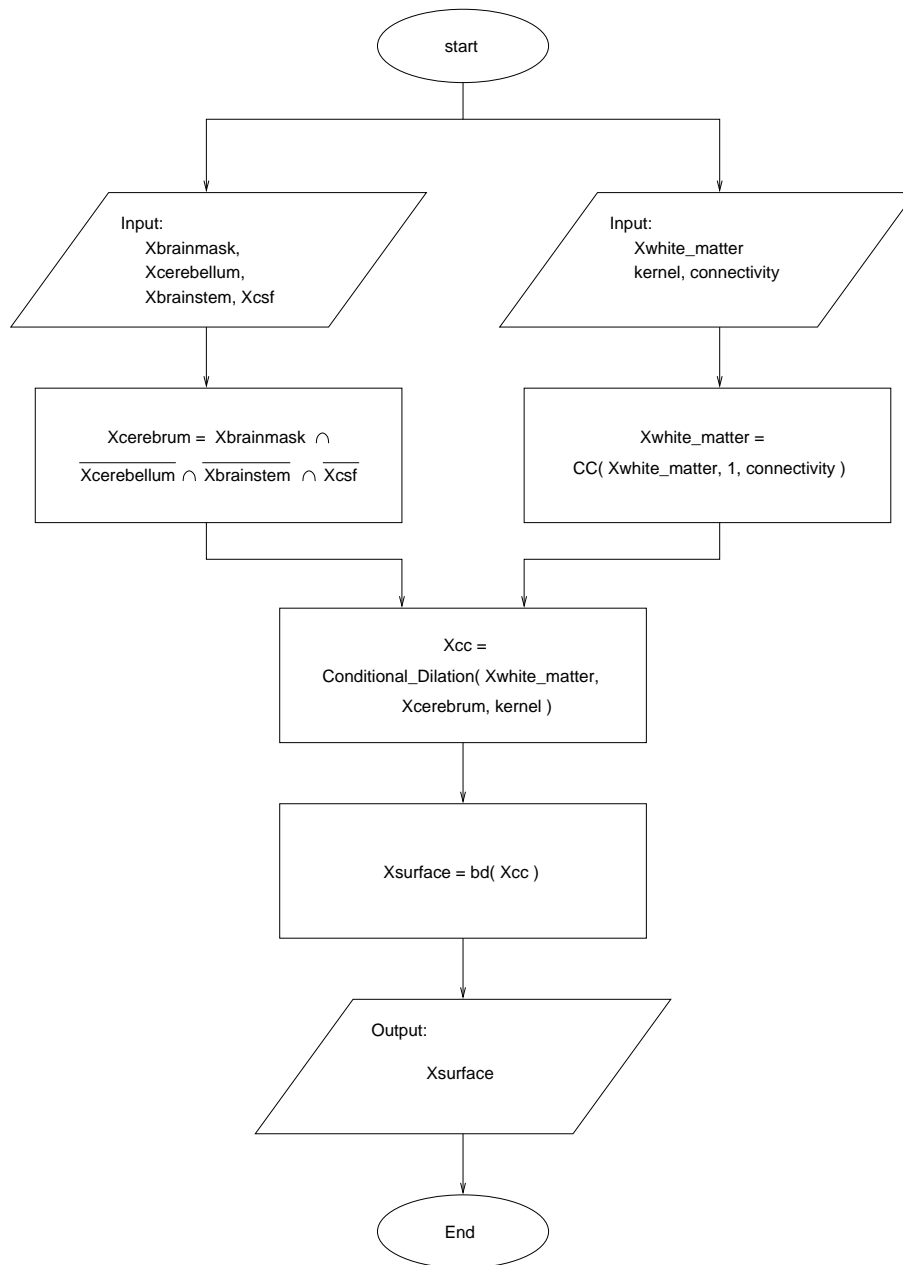


Figure 4.3: Flowchart of the procedure to obtain the cortical surface

Chapter 5

Results

5.1 Experimental results

In figures 5.1 and 5.2 twelve axial slides are shown. The first slide is the lowest one. The distance between the slices is 6 millimetres. The cortical surface is represented by red closed contours. Since the cortical surface is a three dimensional object, there may appear small circular contours in the slide that seem to be disconnected from the bigger contour. They are of course not disconnected, but connected in the third dimension, perpendicular to the slide. This can also be understood if one considers e.g. figure 5.3.

In figures 5.3 and 5.4 three dimensional representations can be found. They are rendered from the same cortical surface that is pictured in figures 5.1 and 5.2.

5.2 Discussion

The quality of the cortical surface depends heavily on the quality of the segmentation of the parts that are taken as input (brain-mask, cerebellum, brainstem, CSF and white matter). If for instance the cerebrospinal fluid is not segmented correctly, the cortical surface that is found by our approach will not have the correct form.

If some surficial voxels were not added during the conditional dilation, then the surface found in our approach will show some distance to the actual cortical surface. However this also assures that the right topology is maintained. In this case preservation of the right topology is chosen over millimetric precision. Yann Cointepas [Coi99] proposes an approach that allows a more precise description of the cortical surface, using cellular complexes. This description, though, makes the treatment of the cortical surface much more difficult, and is not very suited for creating a mesh.

If these constraints are taken into account, the approach has proven to be very robust. Since our approach delivers a volumic representation of the cortical surface, with the topology of a hollow sphere, it might be very suitable for creating a mesh representation of the cortical surface.

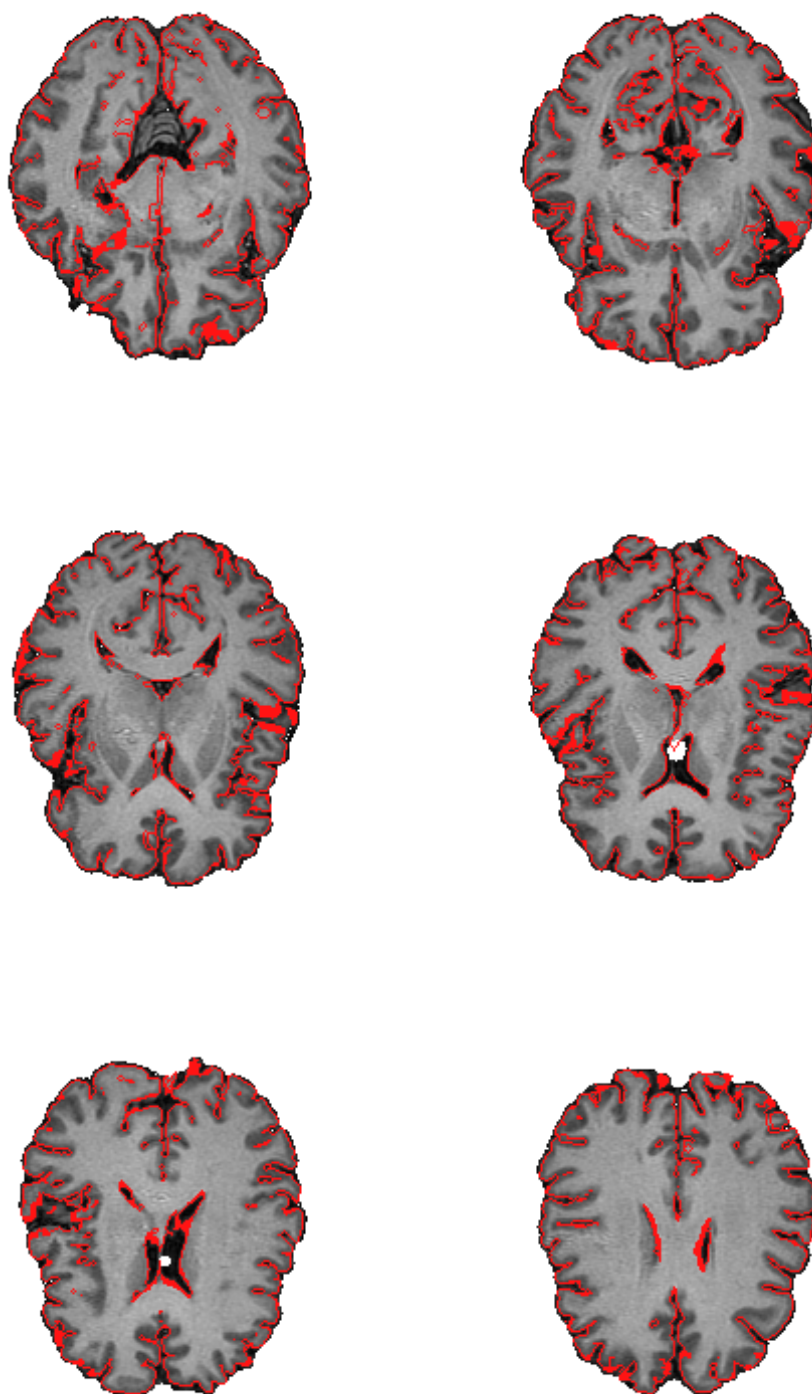


Figure 5.1: The cortical surface, lower slides

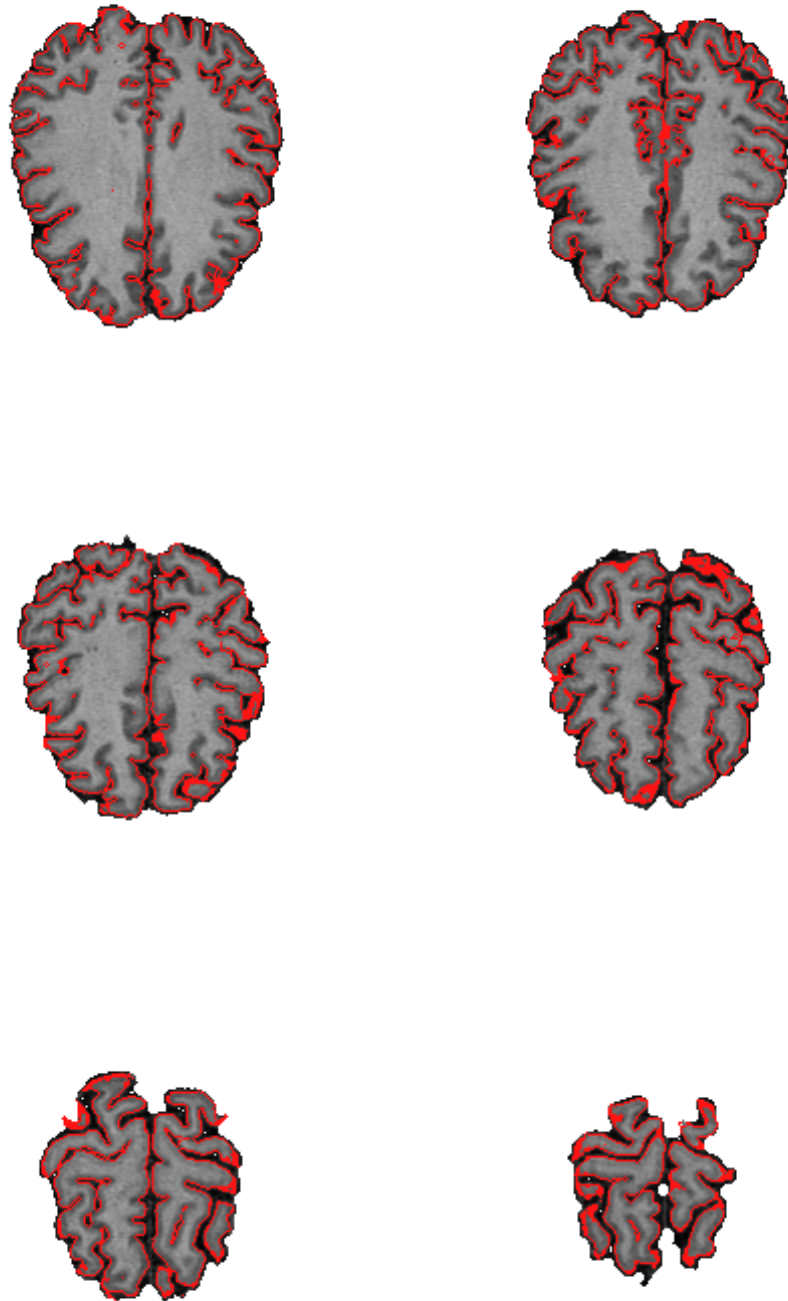


Figure 5.2: The cortical surface, upper slides

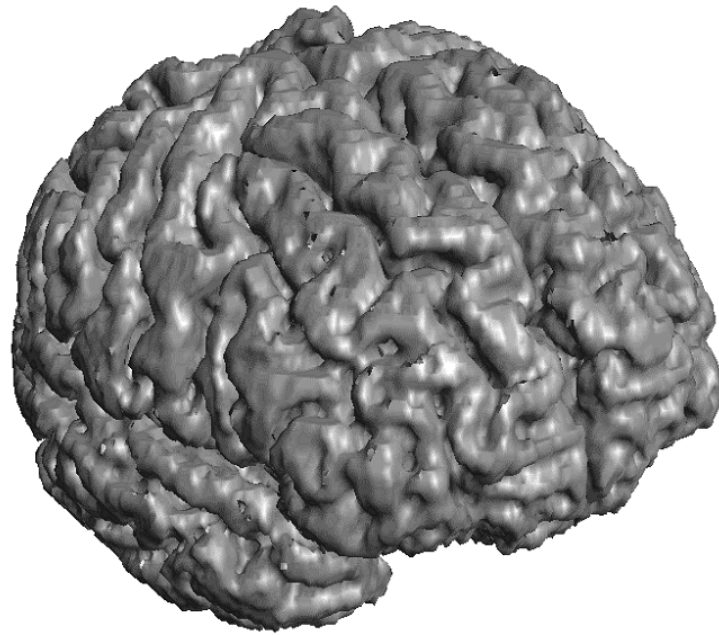


Figure 5.3: 3D representation of the cortical surface, upper front view

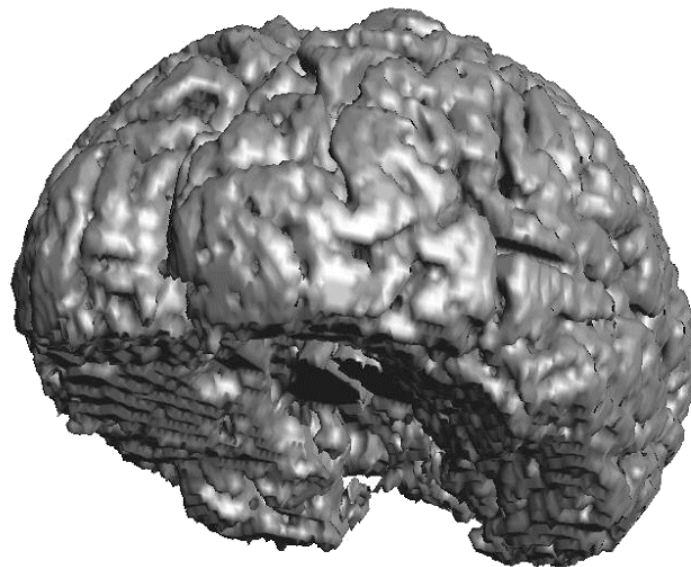


Figure 5.4: 3D representation of the cortical surface, lower view

Part II

Separation of the hemispheres

“Gentlemen,

One cannot but be struck by a comparison of the following facts. First, the cerebral hemispheres, the higher part of the central nervous system, is a rather impressive organ. In structure it is exceedingly complex, comprising millions and millions (in man - even billions) of cells, i.e., centres or foci of nervous activity. These cells vary in size, shape and arrangement and are connected with each other by countless branches. Such structural complexity naturally suggests a very high degree of functional complexity. Consequently, it would seem that a boundless field of investigation is offered here for the physiologist. Secondly, take the dog, man’s companion and friend since prehistoric times, in its various roles as hunter, sentinel, etc. We know that this complex behaviour of the dog, its higher nervous activity (since no one will dispute that this is higher nervous activity), is chiefly associated with the cerebral hemispheres. If we remove the cerebral hemispheres in the dog (Goltz and others), it becomes incapable of performing not only the roles mentioned above, but even of looking after itself. It becomes profoundly disabled and will die unless well cared for. This implies that both in respect of structure and function, the cerebral hemispheres perform considerable physiological work.”

Ivan Petrovich Pavlov, Lecture on the Cerebral Hemisphere[Pav57], 1924

Chapter 6

The hemispheres

The cerebrum, also called forebrain, is the biggest part of the human brain. It consists of two halves called the cerebral hemispheres, and hosts the major higher brain functions. The hemispheres, lying very closely to each other, are separated by the *fissura longitudinalis cerebri*. Only in the centre they are connected by the corpus callosum.

Although there is an approximate symmetry between left and right cerebral hemispheres (for example, there are two occipital lobes, two parietal lobes and there are two frontal lobes), this symmetry is not exact. By the end of the 19th century scientists started to discover that each hemisphere is specialized in performing certain tasks. For instance, for most people the left hemisphere, which manages the right side of the body, controls language and general cognitive functions. The right hemisphere, controlling the left half of the body, manages nonverbal processes, such as attention, pattern recognition, line orientation and the detection of complex auditory tones.

Even though the two hemispheres have different functions they do not work independently of each other. They communicate back and forth across the corpus callosum, each acting as independent parallel processors with complementary functions. This is not an equal partnership however; one hemisphere usually dominates over the other, an effect best illustrated by the fact that most people have a preference using either their left or their right hand. In most cases the left hemisphere is believed to be the dominant hemisphere, and consequently the right hand the preferred hand.

6.1 Separation of the hemispheres: state of the art

Before separating the hemispheres, first the set of voxels that form the brain (the brain mask) are determined, and the brain tissues, such as grey matter, white matter and cerebrospinal fluid (CSF) are identified, just like when segmenting the cortex (see section 3.1). Because the *cerebral* hemispheres are supposed to be separated, the discrimination between the large brain structures such as the cerebrum, the cerebellum and the brainstem is often made in a preliminary step.

Mid-sagittal plane Several authors have described various techniques to separate the hemispheres making use of the so-called mid-sagittal plane. This plane is defined as the plane that best fits the inter-hemispheric fissure of the brain (fissura longitudinalis) [MGS⁺96], or as the plane that maximizes similarity between the image and its reflection relative to this plane [LCR98, PTSR98]. A disadvantages of these approaches is that the boundary between both hemispheres is not planar. Further is the symmetry between both hemispheres never perfect, and the degree of symmetry between them can vary from individual to individual.

Template matching Maes *et al* [MVLD⁺99] propose a method to separate both hemispheres using template matching. After bias correction and tissue classification, left and right hemispheres are separated by non-rigid registration to a template image in which both hemispheres have been carefully segmented. With this method it is uncertain how well the hemispheres are separated if their morphology differs considerably from the template image.

6.2 Research question

The second objective set for this thesis is the morphological separation of the both cerebral hemispheres. Since each hemisphere hosts different functions, it can be of interest to study brain activity when performing different tasks, and identify the distribution of functionality between the hemispheres. The possibility to access the volumes of each hemisphere in MRI images allows the examination of back-projected EEG and MEG signals separately for each hemisphere. Of course having both the volumes of the hemispheres allows also the inter-individual study of the morphology of both hemispheres. Also in case of a pathology it may be of interest to access each hemisphere separately.

6.3 Limitations and difficulties

The two hemispheres are separated by the fissura longitudinalis cerebri, a very deep and narrow furrow. Due to the resolution of the MRI technique, which is currently in the order of one cubic millimetre, sometimes convolutions that lie at opposite sides of the fissura longitudinalis cerebri seem to grow together. They are in fact not really connected, but the space between them is too small to appear in the MRI image, due to the partial volume problem (see section 3.3).

The hemispheres are physically connected by the corpus callosum. The division within the corpus callosum of which voxels belong to the right hemisphere, and which ones to the left hemisphere, is somewhat arbitrary.

Chapter 7

Approach

The approach presented here is based on the idea to erode the volume representing the cerebrum (the forebrain), in order to obtain two marker volumes, one situated in the left hemisphere, and the other in the right hemisphere. Henceforth the two marker volumes are dilated simultaneously, until they meet each other, or the bounds of the cerebrum is reached. During this dilation, the dilated marker volumes will each remain their own value, and we will end up with two marked volumes, together filling up the cerebrum. The flowchart of this procedure can be found in figure 7.1.

7.1 Marker volumes: erosion of the cerebrum

In order to obtain the marker volumes the cerebrum is eroded first a number of times. As erosion kernel we chose the N_{18} kernel, because this kernel is a better approximation of the Euclidean ball than for instance the N_6 or N_{26} kernels, and thus produces a more “rounded” eroded object than those kernels. The number of times the erosion is performed is determined by the variable n in the flowchart in figure 7.1. We performed our tests with n set to 3.

After the cerebrum is eroded blindly, we test whether the hemispheres are really separated. From the image, gained as a result of the erosions, the two largest connected objects are taken. If the hemispheres were not separated, then the largest simply connected object simply consists of the two, still connected, markers. The second largest object is a group of voxels, disconnected because of the erosion operation. The volume of these objects (the number of voxels they consist of) differs considerably. Therefore we conclude that if their volume is within a certain range, the hemispheres are separated and we may proceed. Otherwise, another erosion is needed. The formula to assess this is

$$\left| 1 - \frac{marker1}{marker2} \right| < maxdif \quad (7.1)$$

Whereby $marker1$ and $marker2$ represent the number of voxels in the first and second largest simply connected component. $maxdif$ is the factor that they are allowed to differ. We chose 0,15 for $maxdif$. It may be noted that it is also very easy to visually check whether the markers are separated.

7.2. PROBLEMS WITH MARKER VOLUMES: GROWING INTO EACH OTHER



Figure 7.1: Flowchart of the procedure to obtain the hemispheres

7.2 Problems with marker volumes: growing into each other

If the distance of one of the markers to the boundary that separates the hemispheres, is smaller than the distance of the other marker to the boundary, then it is possible that during the dilation

voxels of one hemisphere will be falsely assigned to the other. One hemisphere will grow into the other, so to speak (see figure 7.2). Of course this can only happen where both hemispheres are connected in the MRI image. They are connected, both in the MRI image and physically, by the corpus callosum. Complementary to that some convolutions lying at opposite sides of the fissura longitudinalis are connected in the MRI image due to the partial volume problem (see sections 3.3 and 6.3).

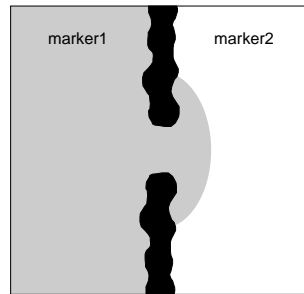


Figure 7.2: Marker1 grows into the other hemisphere

Because the erosion will have the same pace for both hemispheres, in most cases the distance of the markers to the boundary will correspond. Though due to the irregular form of the hemispheres the form of the markers is also quite rough, and therefore the markers do not always have the same distance to the boundary. However during the dilation stage the furrows in the markers will be closed, and then the “growing into each other” is often prevented. The dilation has a “smoothing” effect on the markers.

A much bigger problem is the case where the side of one hemisphere is much wider than the other. Then it is possible that for the narrow hemisphere the marker is totally eroded away at that side, and the marker of the wider one is not. If both hemispheres are connected in the MRI image at such a side, then it is very likely that there one will “grow into the other”. To deal with this problem we *justify* the markers. We developed two approaches to justify the markers.

7.2.1 Justification: rectangular markers

For this approach we substitute the markers with rectangular volumes. We assume the markers to be positioned beside each other in the direction of one axis (for instance in x -direction). The rectangular volumes have the same dimensions as the maximal dimensions of the original marker volumes. For the other two Cartesian directions (for instance y - and z -direction) the both rectangular markers have the same dimensions. In these directions they assume the least of the maximum position of either of both original markers. Further it is possible to subtract a constant from each measure.

This method solves the problem of cases that have the side of one hemisphere wider than that of the other hemisphere. Also after the dilation the cut between the hemispheres is very straight, because of the form of the rectangular markers. This results particularly in a nice straight cut in the corpus callosum (see e.g. figure 8.10). However this method totally disregards the form

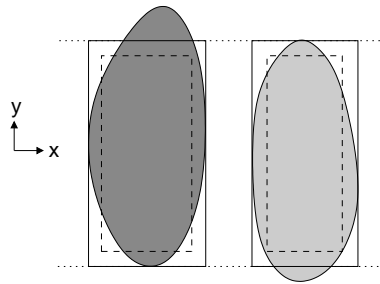


Figure 7.3: Rectangular markers

of fissura longitudinalis, And therefore the chance of one hemisphere “growing into the other” is much larger. Especially when the boundary between the hemispheres is not more or less a straight plain, but is bended in one or more directions.

7.2.2 Justification: intersection of the markers

Again we assume the markers to be positioned beside each other in the direction of one axis (for instance in x -direction). Now we consider every scanline in this direction. Only if *both* markers have voxels in this scanline, they are included. This has the effect that the markers are intersected for the other dimensions (y, z in the example).

This method follows the form of the fissura longitudinalis, and is not sensitive for brains that have the side of one hemisphere broader than that of the other hemisphere. However the cut in the corpus callosum is not so straight (see e.g. figure 8.11). Since the assignment of voxels to one hemisphere or the other within the corpus callosum is somewhat arbitrary anyway, this might be regarded as a cosmetic problem (a certain division might look better, but is not necessarily evaluated as being better).

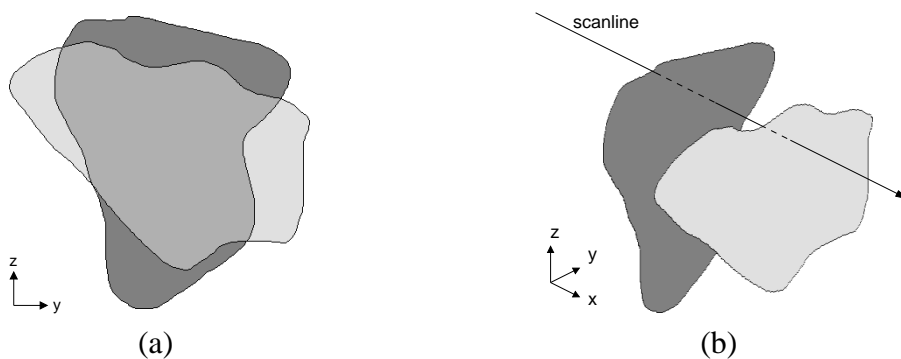


Figure 7.4: (a) Intersection of markers in y, z (b) scanline in x -direction

7.3 Multiple dilation

After the marker volumes are obtained, we have two volumes. One consists of simply connected voxels, that all have the value “1”, and the other is formed by simply connected voxels, that all have the value “2”. Now they will be dilated simultaneously. Hereby voxels are only added if they are 1. in the volume of the cerebrum, and 2. they are not already added to the other marker. The added voxels are assigned the value of the marker they are added to. Thus, they will be assigned either the value “1” or “2”. This dilation will be repeated until there are no more voxels that can be added. As dilation kernel the same kernel as for the erosion is used (N_{18}), in order to retrace the original form as much as possible. As a result we will have two volumes, marked “1” and “2”, together filling up the entire cerebrum.

7.3.1 Meeting markers

If during the multiple dilation the two marker volumes would meet, meaning they reach the same position at the same dilation step, it could be possible that one marker grows diagonal over the other, if this marker always would be dilated first (see figure 7.5a). This would be the case if we use a “miss or hit” operation, and scan the volume always in the same direction. To prevent this from happening we scan our volume alternating in increasing and decreasing direction. Thus we first use a loop starting with the smallest x , y and z , and increment them. And then use a loop starting with the maximal x , y and z , and decrement them. In case of meeting marker volumes this leads to result illustrated in figure 7.5b. If a N_6 dilation kernel is used, the effect of figure 7.5a cannot happen, the markers just would grow vertically.

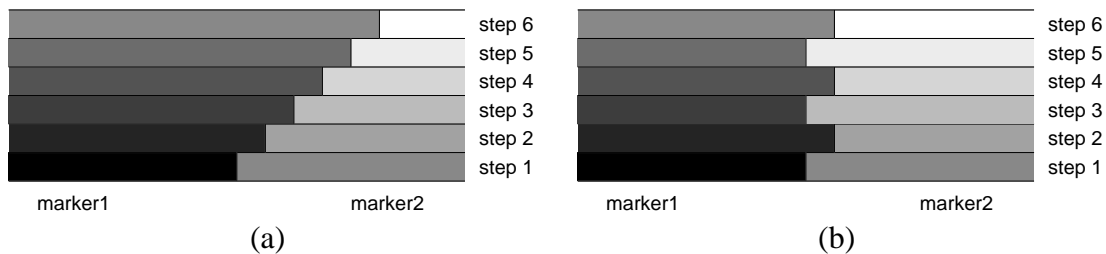


Figure 7.5: Meeting markers: (a) stair effect, (b) zigzag effect

Chapter 8

Results and discussion

8.1 Experimental results

In figure 8.2 unjustified marker volumes are shown, that were obtained according the procedure described in chapter 7. In figure 8.3 the corresponding separated hemispheres are shown that resulted from the multiple dilation. For this particular MRI the separation was untroubled, even with the unjustified markers. In figure 8.1 a three dimensional representation of the two separated hemispheres can be found.

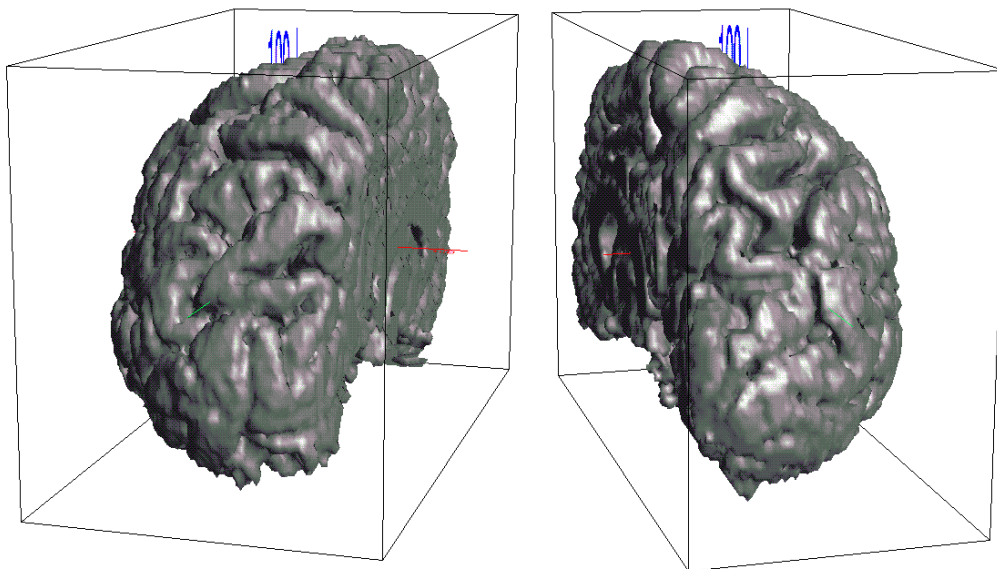


Figure 8.1: The separated hemispheres in 3D

8.2 Limitations and difficulties

In figure 8.5 we find a good example of a marker that grew into the other hemisphere (see also section 7.2). The reason for this phenomenon can be found in figure 8.4; the left marker is still present in the lower region of the left hemisphere, where the right marker is completely eroded away at the corresponding region in the right hemisphere.

The first solution to tackle this problem is shown in figure 8.6. These markers were created from the original markers in figure 8.4 according to the method described in section 7.2.1, with the border constant set to 5 voxels. The result of the multiple dilation of these markers can be found in figure 8.7. As is clearly visible, the markers do not grow in the other hemispheres.

In figure 8.8 the second solution is shown; the markers are justified by intersecting them (see section 7.2.2). If figure 8.8 is compared to figure 8.4, we can see that the lower part of the original left marker has been removed. The result of the multiple dilation of these markers can be found in figure 8.9. Because the part of the left marker that caused it to grow into the right hemisphere has been removed, the problem of growing into the hemisphere has been lifted.

8.3 Discussion and prospects

The rectangular markers deliver a very straight cut between the two hemispheres, as can be seen in figures 8.7 and 8.12. This can be of advantage when searching a straight plane between the hemispheres. Also, the corpus callosum is visually more apparent in a three dimensional representation. This is plain when figure 8.10, obtained with rectangular markers, is compared with figure 8.11, obtained with intersected markers. However that does not mean that the separation in the corpus callosum is better when using the rectangular markers, only visually more plain. The division between the two hemispheres within the corpus callosum is somewhat arbitrary, and therefore one could argue that different separations are valid.

The rectangular markers meet their limitations when the fissura longitudinalis is bended in one or more directions. They assume the bounds between the hemispheres to be quite straight, and when that is not the case the separation provided by the rectangular markers will contain errors. This problem does not exist for the intersected markers. They follow the form of the fissura longitudinalis, as it is provided by the erosion, and just remove the parts of the markers that may cause the growing into the other hemisphere.

The procedure, with the different justified markers, applied on MRI images has proven to be very robust. However, for some MRI images the assignment of a small number of voxels arguably may be ambiguous. However it should be noted that the precise anatomical division between the two hemispheres is rather subjective. A possible approach for future investigations might be a separation based on dynamical surfaces (snakes), which possibly could take the division obtained by the approach described in this thesis as a starting point.

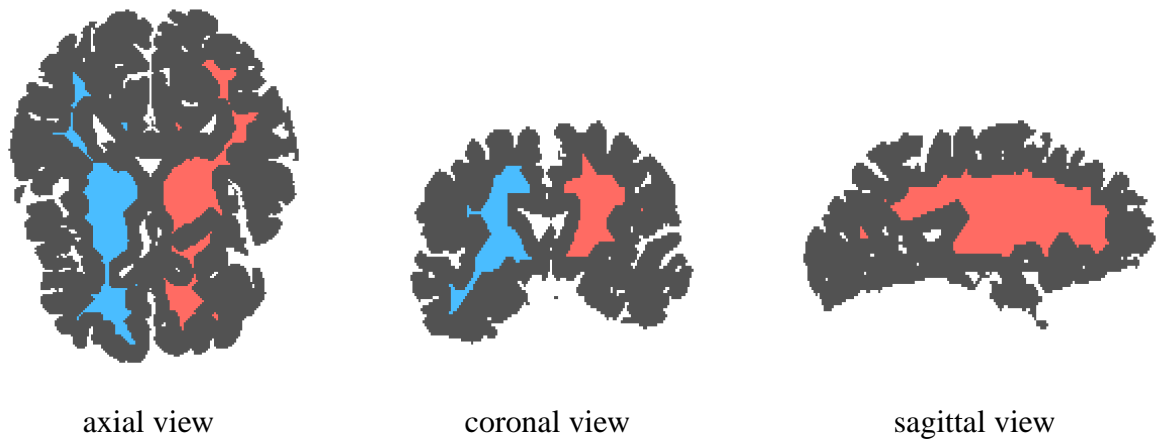


Figure 8.2: Unjustified marker volumes

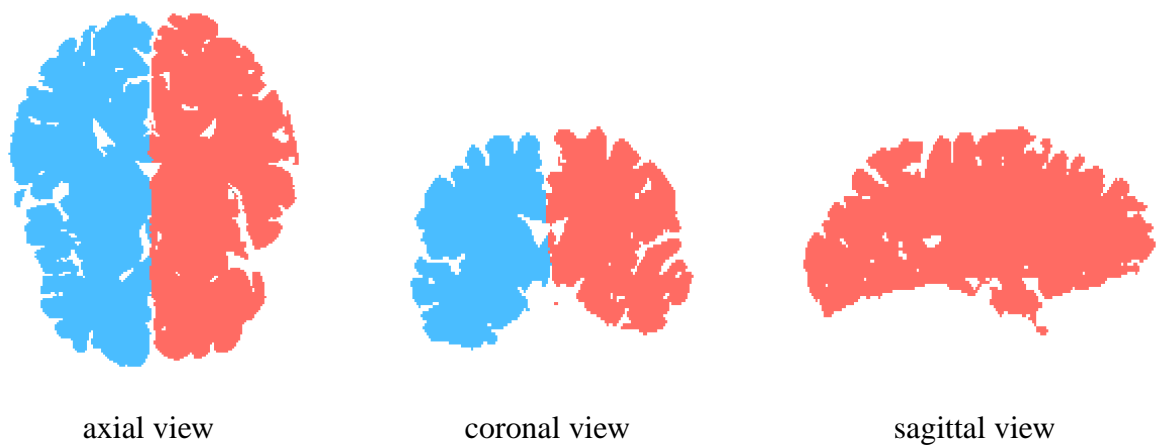


Figure 8.3: Separated hemispheres, obtained from unjustified markers

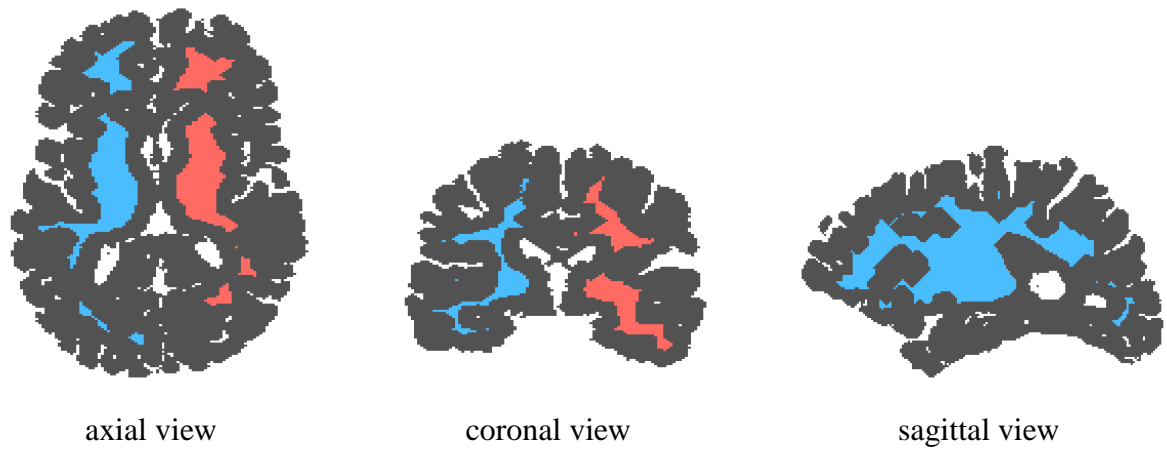


Figure 8.4: Example of unjustified marker volumes

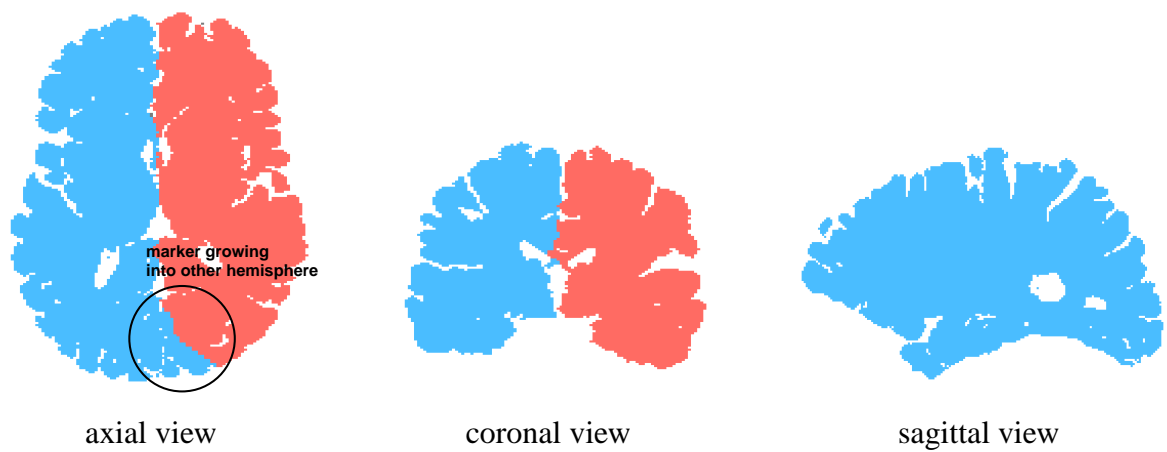


Figure 8.5: Example of a marker that grew into the other hemisphere

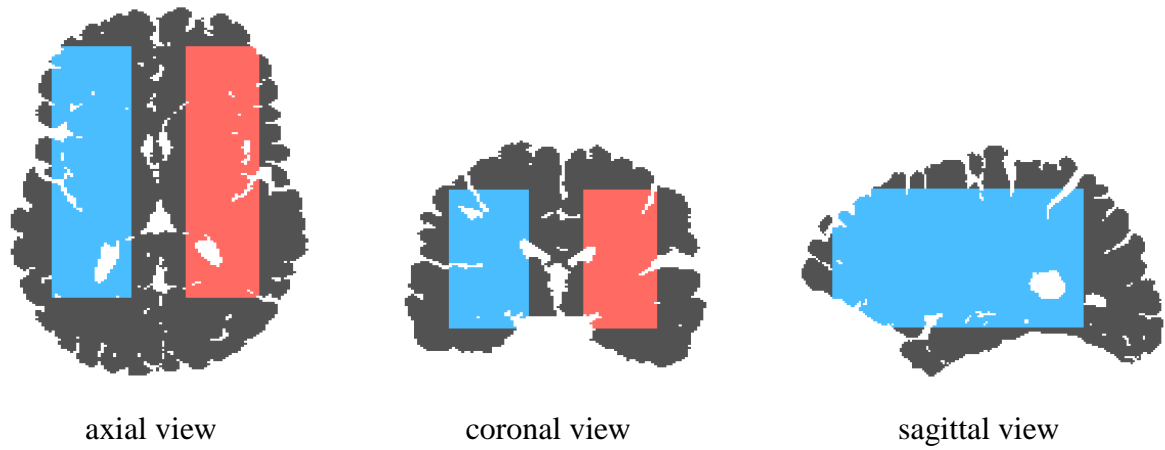


Figure 8.6: Rectangular marker volumes

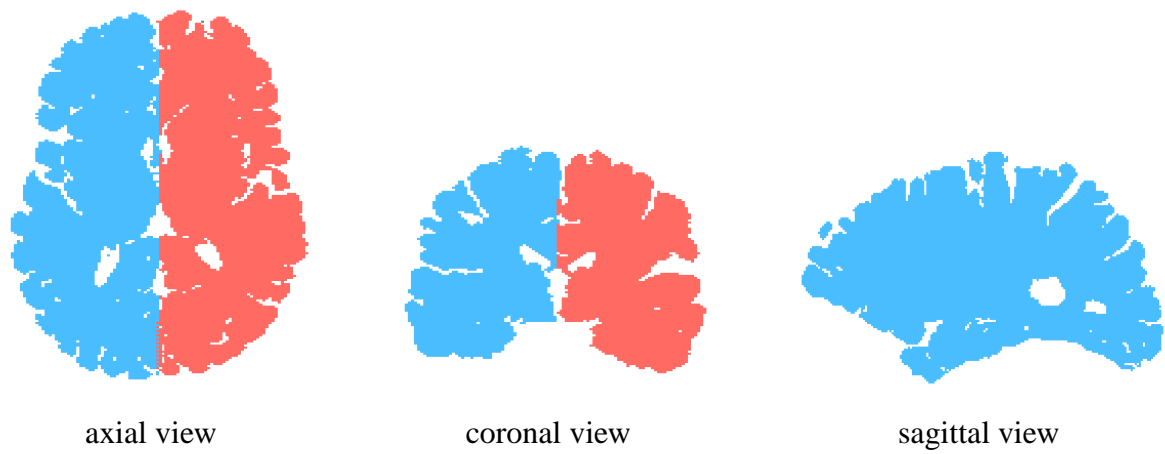


Figure 8.7: Separated hemispheres, obtained from rectangular markers

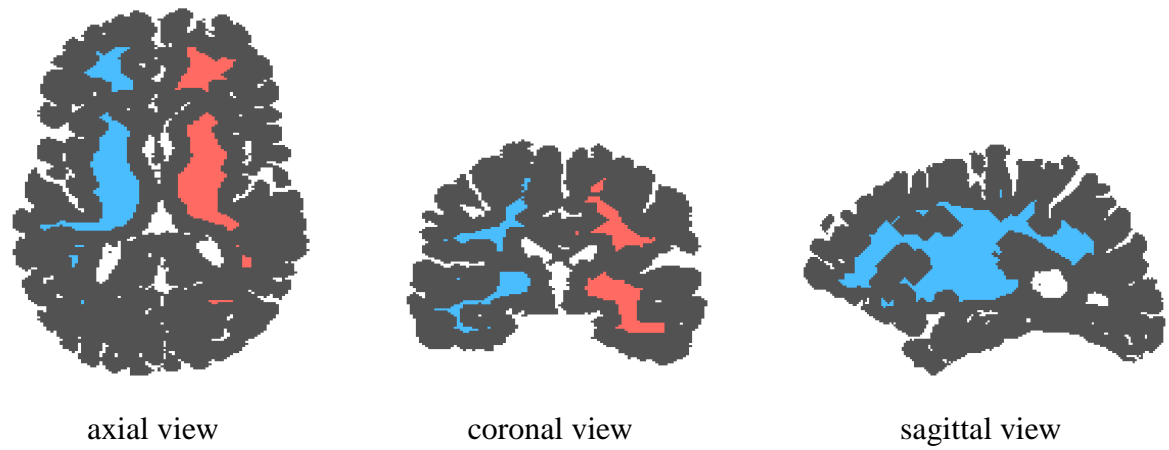


Figure 8.8: Intersected marker volumes

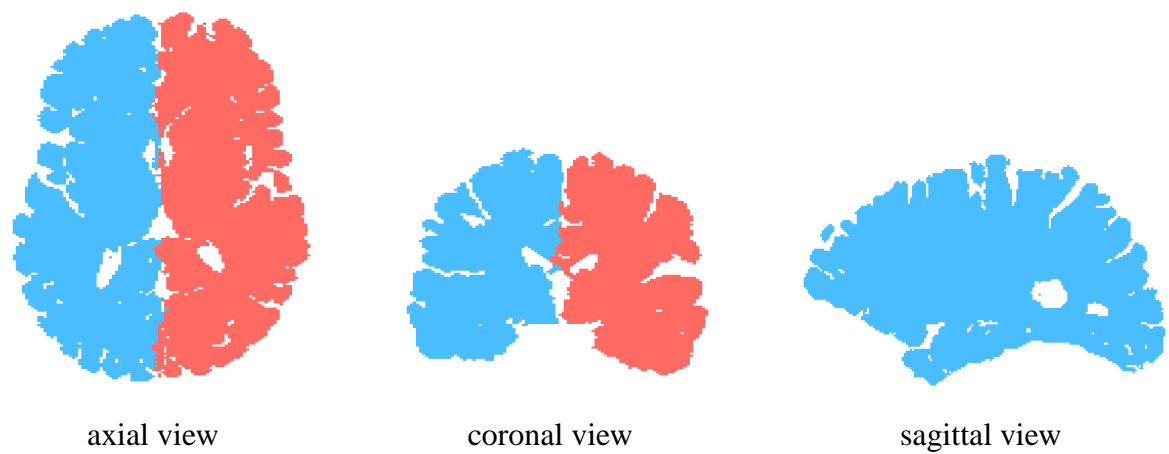


Figure 8.9: Separated hemispheres, obtained from intersected markers

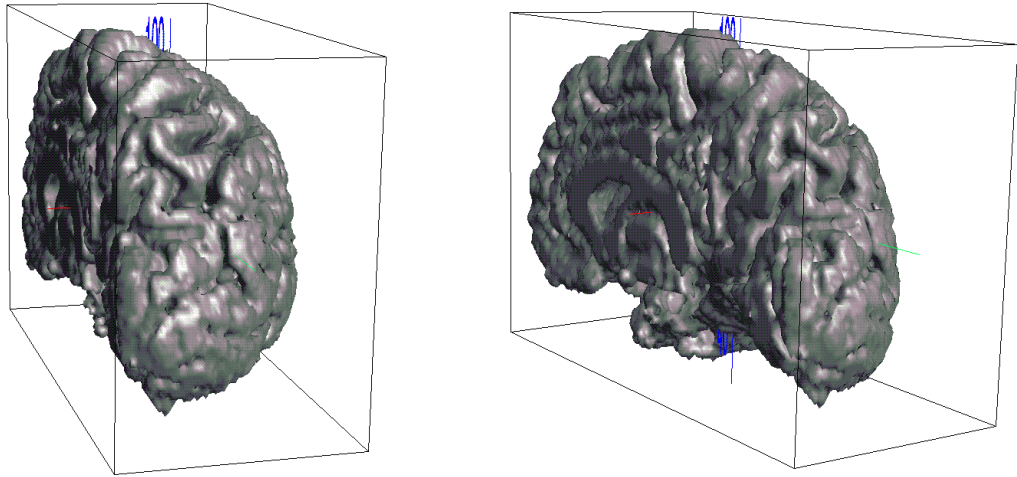


Figure 8.10: 3D representation of a hemisphere (pictured under two different angles), obtained with rectangular markers

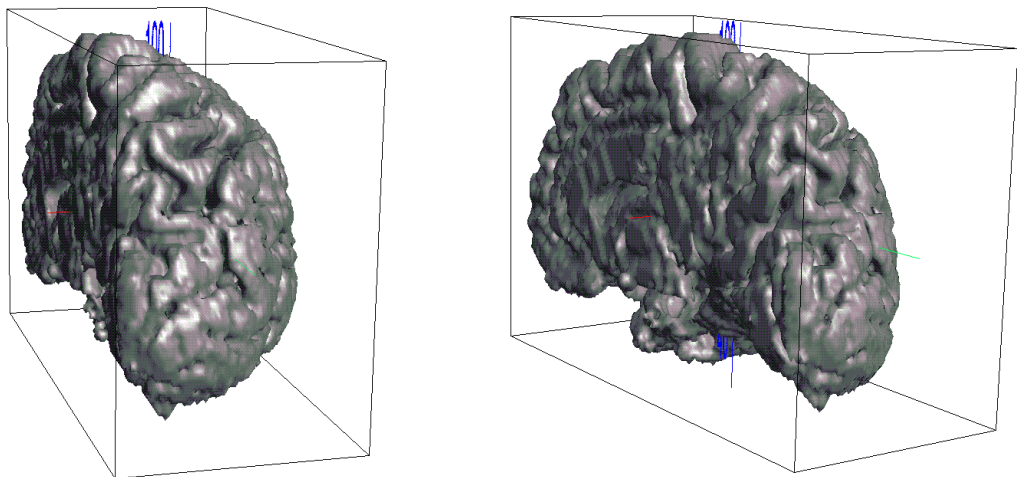


Figure 8.11: 3D representation of a hemisphere (pictured under two different angles), obtained with intersected markers

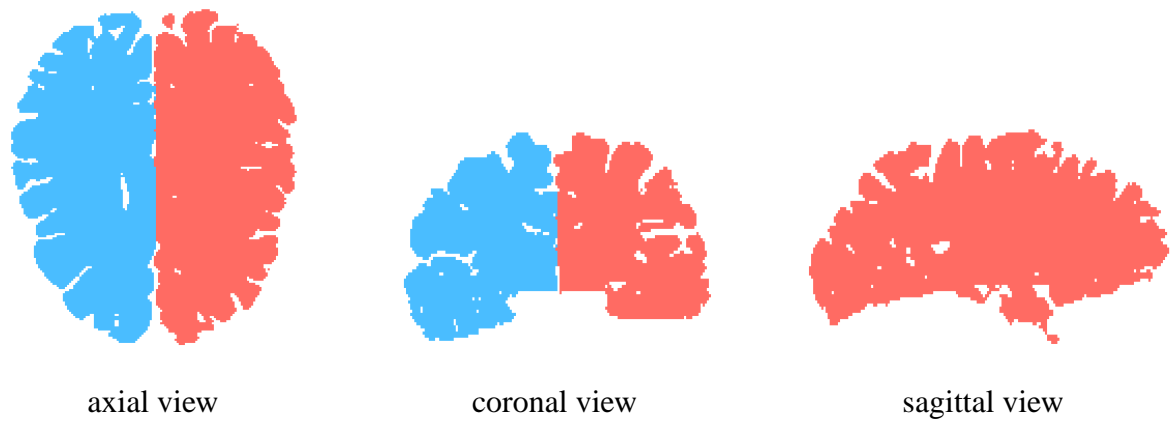


Figure 8.12: Separated hemispheres, obtained from rectangular markers

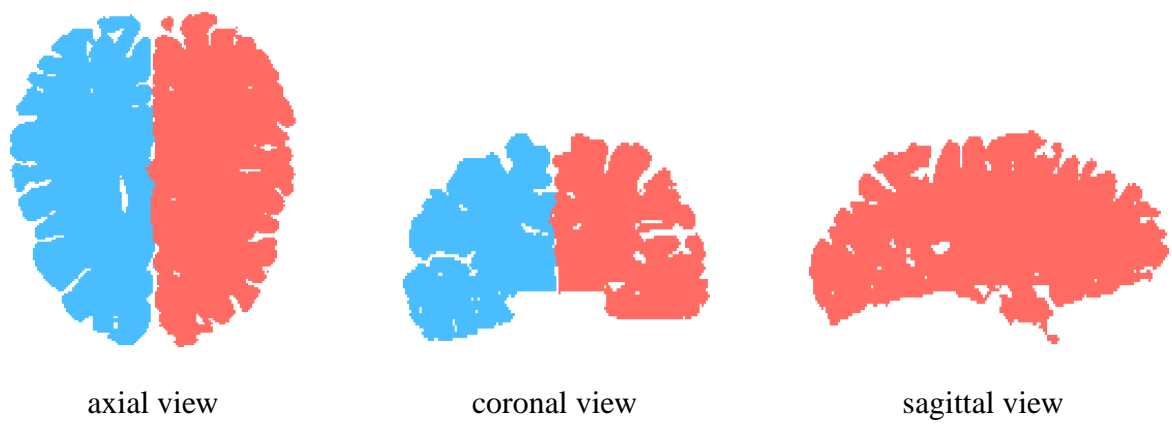


Figure 8.13: Separated hemispheres, obtained from intersected markers

Chapter 9

Conclusion

Objectives for this thesis were the extraction of the cortical surface and the morphological separation of both hemispheres. Since this thesis is part of a larger project (see section 1.1) some anatomical parts of the brain could be assumed to be already segmented (see section 4.1). Procedures to meet these objectives have been developed. Several modules necessary to run these procedures have been implemented in C++ routines. The taken approaches are heavily based on mathematical morphology. The MRI images, used in our tests, were provided by the LENA Salpêtrière Hospital in Paris. They were normal MRI images from usual quality, taken from different human subjects.

9.1 The cortical surface

In order to extract the cortical surface, we started with a simply connected volume, representing the white matter. This volume was dilated under the condition that voxels were only added if 1. the resulting volume would be still simply connected, 2. they were positioned within the cerebrum. The cerebrum was defined as the brain-mask with the cerebellum, the brainstem and the CSF subtracted. This dilation was continued until there were no more voxels left to be added. We would end up with a simply connected volume with an outline corresponding to the cortical surface. The internal surface of this volume would be taken as end result: the cortical surface.

One of the major conditions we impose on the extraction of the cortical surface is that the result has to have the topology of a hollow sphere. This condition is imposed in order to be able to project signals measured on the scalp, such as MEG and EEG, on the cortical surface (inverse problems). Though the real cortical surface does indeed have this topology, it is often compromised in MRI images because of the partial volume problem (see section 3.3). The chosen procedure opens closed cavities, and by doing so, it assures the required topology. Though millimetric precision is not always reached by this approach, the preservation of the right topology was valued higher.

The quality of the extraction of the cortical surface depends very much on the quality of the segmentation of the parts that are taken as input (brain-mask, cerebellum, brainstem, CSF

and white matter). If for instance the cerebrospinal fluid is not segmented correctly, the cortical surface that is found by our approach will not have the correct form.

If these constraints are taken into account, the extraction of the cortical surface has proven to be very robust. For all the images that have been tested, the surface has been found without any problems. The volumic representation of the cortical surface with the topology of a hollow sphere, which is delivered by our approach, might be a good starting point for construction of a mesh representation of the cortical surface.

9.2 The hemispheres

The approach to separate the hemispheres has been based on the idea to erode the volume representing the cerebrum (the forebrain), in order to obtain two marker volumes, one situated in the left hemisphere, and the other in the right hemisphere. After obtaining the two marker volumes, they were dilated simultaneously, until they met each other, or the bounds of the cerebrum is reached. During this dilation, the dilated marker volumes would each remain their own value, and we end up with two marked volumes, together filling the cerebrum.

The major disadvantage of this method is that there is a possibility that one marker volume grows into the other hemisphere (see section 7.2). The risk of this happening is especially present in the case that at some height one marker volume has been eroded away completely, and the other marker volume has still voxels left at the corresponding height. To deal with this problem we have developed two different solutions. The first solution is to justify the marker volumes by creating rectangular markers from the original ones, and the other is to justify them by intersecting the two markers in the direction they are positioned beside each other (see sections 7.2.1 and 7.2.2). These solutions have proven to solve the problem substantially.

The separation that is delivered by our approach might form the starting point for fine-tuning of the separation based on different criteria. A possible future project could be based on the application of dynamical surfaces (snakes) in the separation of the cortical hemispheres.

Appendix A

Implementation of the algorithms

A.1 introduction

The MRI scans were stored in files, characterized by a “.ima” extension, containing the raw data (no header information) as a string of bytes, whereby every byte represents a gray level value. The string can be interpreted as a three dimensional voxel image in the following way:

```
for (z = 0 to MAX_Z - 1)
  for (y = 0 to MAX_Y - 1)
    for (x = 0 to MAX_X - 1)
      {
        BYTE[x][y][z]
      }
```

The dimensions (MAX_X , MAX_Y and MAX_Z) of the image are stored in an accompanying file, with a “.dim” extension. This file also contains the physical dimensions of a voxel.

The procedures, as shown in the flowcharts in figures 4.3 and 7.1 were implemented in c shell scripts. They can be easily executed by entering at the Unix command-line: “corticalsurface.sh MRIimage”, and respectively “separate_hemispheres.sh MRIimage”, whereby the “MRIimage” is the filename of the MRI image without extensions. In the shell scripts it is documented which names the pre-segmented parts that are taken as input, are supposed to have. From the shell scripts the various modules are executed.

To implement the different modules of our procedures we make use of the *Tivoli* library, a set of C++ routines and binaries. The algorithms, which were not provided by the Tivoli library, were developed for this project in C++. They were: the conditional dilation, the justification of the marker volumes; rectangular markers, and intersected markers, and the multiple dilation. We will give a brief description of those algorithms in the following sections.

A.2 The conditional dilation

The conditional dilation plays a major role in the cortical surface extraction (see chapter 4). In this section the implementation of this conditional dilation is described.

As input parameters an *image* that contains the to-be-dilated object, a *mask image* and the *dilation kernel* (N_6 , N_{18} , or N_{26}) are taken. The first condition that is imposed on the dilation, is that a voxel is only added if it is within the mask. A voxel is within the mask if the mask image has a non-zero value on the corresponding position. The second condition is that it is a simple point (see definition 4.1).

A.2.1 distance transform

The conditional dilation is implemented in two steps. First a distance transform (see section 2.5) is applied on the input image into the mask. For the distance transformation (DT) we also refer to [Bor86, Ver91]. In our application this means that the distance transform is performed the volume of the white matter into the cerebrum. Thus the white matter will have distance 0, in the cortex the value increases in direction of its bounds, and the volume outside the cerebrum is filled with the maximum value (255). This is visualized in figure A.1.

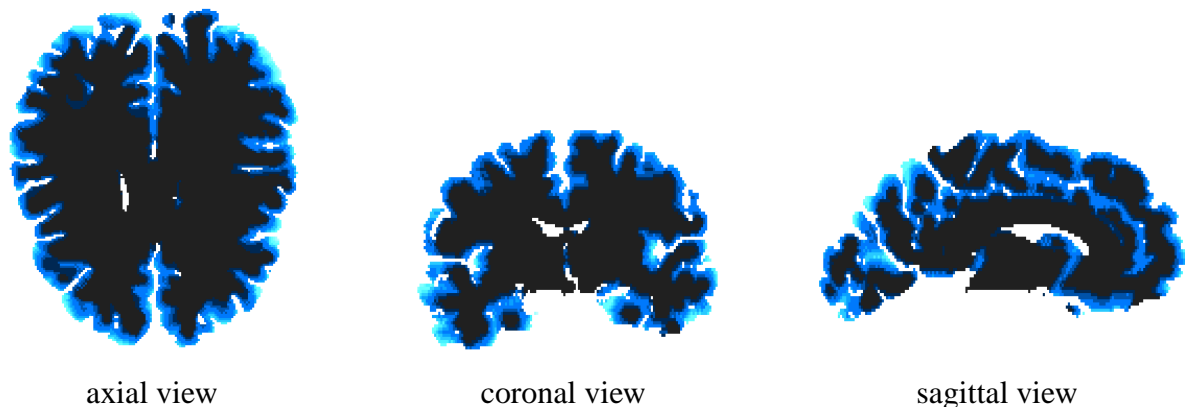


Figure A.1: Distance transformation of the white matter into the cerebrum

A.2.2 priority waiting list system

For the second stage of the implementation the distances are regarded as priorities, whereby the smallest distance has the highest priority. All simple points of the highest priority are added to the object from the input image. The non-simple points are put in a waiting list system.

The waiting list system contains a queue for every priority. In order to initialize the queues a histogram is made of the image with the priorities. The queues are given the size of the number of voxels of the corresponding priority, so if all voxels of a given priority were put in the waiting list system, the queue of that priority would be completely filled.

A.2. THE CONDITIONAL DILATION

Now we descend one priority, and proceed with adding all simple points, and putting the resting voxels of that priority in the waiting list. Then the voxels in the waiting list are checked whether they still are not simply connected, starting with the queue of the highest priority, and then descending. This is necessary because it is possible that voxels that were previously non-simple, now are simple points, as a result of surrounding voxels that have been added to the object. This procedure is repeated, until all distances, except for the maximum distance (the voxels outside the cerebrum), are dealt with.

```
input:  image, mask_image, kernel
output: image

dist_image = DT(image, mask_image)
histo = Histogram(dist_image)
queues = InitQueues(histo)

integer dist = 1

do
{
  if (histo[dist] != 0)
  {
    AddSimplePoints(image, dist_image, dist)
    QueueRest(queues, dist_image, dist)
    CheckQueues(image, queues)
  }

  dist = dist + 1
}
until(dist == 255)
```

A.3 Justification of the marker volumes

We assume that the orientation of the brain is more or less aligned with the direction of one of the axis of the reference frame (a small deviation is allowed). As a consequence, the markers are also separated along one axis of the reference frame. Before we justify the markers, we first search the direction in which they are beside each other. In order to determine that direction, we search the minimum and maximum dimensions of both markers, and then search for the direction in which the maximum of one marker is smaller than the minimum of the other. Of course this is only allowed for one direction. For the following sections we assume that both markers are beside each other in x -direction. The corresponding routines for y - and z -orientation can be easily derived.

A.3.1 Creating rectangular markers

After the minimum and maximum dimensions of both markers are determined, the construction of the rectangular markers is quite straightforward. In y - and z -direction the largest of the minima are taken, and the smallest of the maxima. In x -direction both markers maintain their minima and maxima. Then from all dimensions a constant border value is subtracted, and thus all parameters for our two rectangular volumes are obtained. See also section 7.2.1.

A.3.2 Creating intersected markers

Again we assume the markers to be positioned beside each other in the direction of one axis (in our example in x -direction). Now we consider every scanline in this direction. Only if *both* markers have voxels in this scanline, they are included. This has the effect that the markers are intersected for the (y,z) -plane. See also section 7.2.2.

```
for (z = 0 to MAX_Z - 1)
  for (y = 0 to MAX_Y - 1)
  {
    for (follow scanline in x-direction)
    {
      if (both markers are present in scanline) then
        the scanline is maintained
      else
        the scanline is erased
    }
  }
}
```

A.4 The multiple dilation

The multiple dilation takes as input parameters a *labeled image*, containing objects, and a *mask image*. The voxels of every object in the input image are supposed to have a value, unique for the object they belong to (e.g. all voxels of one object have the value “1”, the voxels of another object have the value “2”, etc.). The multiple dilation performs a dilation, with a given kernel (N_6 , N_{18} or N_{26}), on the objects in the image, whereby by the added voxels take the value of the object they are added to. Hereby voxels are only added if 1. they are in the volume of the mask, and 2. they are not already added to an other object. This dilation is repeated until there are no voxels left anymore that can be added to an object.

input: *image*, *mask_image*, *kernel*
output: *destination_image*

```
destination_image = image
do
{
  integer added = 0
  for (z = 0 to MAX_Z - 1)
    for (y = 0 to MAX_Y - 1)
      for (x = 0 to MAX_X - 1)
        {
          if (image[x][y][z] != 0) then
            {
              for (walk through all kernel offsets: kx, ky, kz)
                {
                  if ((mask_image[x + kx][y + ky][z + ky] != 0) and
                      (destination_image[x + kx][y + ky][z + ky] == 0)) then
                    {
                      destination_image[x + kx][y + ky][z + ky] = image[x][y][z]
                      added = added + 1
                    }
                }
            }
        }
      image = destination_image
    }
  until (added == 0)
```

It should be noted, that the actual implementation scans the image alternating in increasing and decreasing direction, to address the problems described in section 7.3.1. Thus we first use a loop starting with the smallest x , y and z , and increment them. And then use a loop starting with the maximal x , y and z , and decrement them. The routine in pseudo-code above scans the volume only in increasing direction though, in order to keep it understandable. In case of a N_6

A.4. THE MULTIPLE DILATION

or N_{18} -kernel, after the routine has finished, we run it with a N_{26} -kernel, in order to add voxels that are still disconnected.

Bibliography

- [Bor86] Borgefors (Gunilla). – Distance transformations in digital images. *Computer Vision, Graphics and Image Processing*, vol. 34, 1986, pages 344–371.
- [Bra89] Bradshaw (John R.). – *Brain Imaging*. – Butterworth & Co., 1989.
- [Coi99] Cointepas (Yann). – *Modélisation homotopique et segmentation tridimensionnelles du cortex cérébral à partir d'IRM pour la résolution des problèmes directs et inverses en EEG et en MEG*. – PhD thesis, Ecole nationale supérieure des télécommunications Paris, France, 1999.
- [DUB01] Dokládal (Petr), Urtasun (Raquel) and Bloch (Isabelle). – Segmentation of 3D head MR images using morphological reconstruction under constraints and automatic selection of markers. *IEEE Int. Conf. on Image Processing ICIP 2001*, 2001.
- [GW92] Gonzalez (Rafael C.) and Woods (Richard E.). – *Digital Image Processing*. – Addison-Wesley publishing company, 1992.
- [Jon92] Jonker (Petrus Paulus). – *Morphological Image Processing: Architecture and VLSI Design*. – PhD thesis, Technische Universiteit Delft, the Netherlands, 1992.
- [LCR98] Liu (Y.), Collins (R.T.) and Rothfus (W.E.). – Automatic bilateral symmetry (mid-sagittal) plane extraction from pathological 3D neuroradiological images. *Proceedings SPIE: Medical Imaging 1998: Image Processing*, vol. 3338, 1998, pages 1528–1539.
- [Mat75] Matheron (G.). – *Random Sets and Integral Geometry*. – Wiley, 1975.
- [MCF98] Mangin (J.-F.), Coulon (O.) and Frouin (V.). – Robust brain segmentation using histogram scale-space analysis and mathematical morphology. *Lecture Notes in Computer Sciences: Proceedings international conference on Medical Image Computing and Computer-Assisted Intervention*, vol. 1496, 1998, pages 1230–1241.
- [ME01] Meyer-Ebrecht (Dietrich). – *Computer-Visualistik Teil B: Bildanalyse*. – Aachen University of Technology (RWTH), Lehrstuhl für Messtechnik und Bildverarbeitung, 2001.

BIBLIOGRAPHY

- [MGS⁺96] Marais (P.), Guillemaud (R.), Sakuma (M.), Zisserman (A.) and Brady (M.). – Visualising cerebral asymmetry. *Lecture Notes in Computer Sciences: Visualization in Biomedical Computing*, vol. 1131, 1996, pages 411–416.
- [Min03] Minkowski (H.). – Volumen und Oberfläche. *Math. Ann.*, vol. 57, 1903, pages 447–459.
- [MVLD⁺99] Maes (F.), Van Leemput (K.), DeLisi (L.E.), Vandermeulen (D.) and Suetens (P.). – Quantification of cerebral grey and white matter asymmetry from MRI. *Lecture Notes in Computer Sciences: Proceedings 2nd international conference on Medical Image Computing and Computer-Assisted Intervention*, vol. 1679, 1999, pages 348–357.
- [Pav57] Pavlov (Ivan Petrovich). – *Experimental Psychology and other essays*. – Philosophical Library, 1957.
- [Pin90] Pinel (John P.J.). – *Biopsychology*. – Allyn & Bacon, 1990.
- [Pra91] Pratt (William K.). – *Digital Image Processing*. – John Wiley & Sons, Inc, 1991.
- [PTSR98] Prima (S.), Thirion (J.-P.), Subsol (G.) and Roberts (N.). – Automatic analysis of normal brain dissymmetry of males and females in MR images. *Lecture Notes in Computer Sciences: Proceedings international conference on Medical Image Computing and Computer-Assisted Intervention*, vol. 1496, 1998, pages 770–779.
- [Ros69] Rosenfeld (A.). – *Picture Processing by Computer*. – Academic Press Inc, 1969.
- [Ros70] Rosenfeld (A.). – Connectivity in digital pictures. *JACM*, vol. 1, 1970.
- [Ser82] Serra (J.). – *Image Analysis and Mathematical Morphology*. – Academic Press Inc, 1982.
- [SHB98] Sonka (Milan), Hlavac (Vaclav) and Boyle (Roger). – *Image Processing, Analysis, and Machine Vision*. – Brooks/Cole Publishing Company, 1998.
- [SM93] Schmitt (Michel) and Mattioli (Juliette). – *Morphologie Mathématique*. – Masson, 1993.
- [TSW97] Teo (P.), Sapiro (G.) and Wandell (B.). – Creating connected representations of cortical gray matter for functional MRI visualization. *IEEE Transactions on Medical Imaging*, vol. 16, 1997, pages 852–863.
- [Ver91] Verwer (Ben J.H.). – Local distances for distance transformations in two and three dimensions. *Pattern Recognition Letters*, vol. 12, 1991, pages 671–682.
- [WFW⁺95] Wagner (M.), Fuchs (M.), Wischmann (H.-A.), Ottenberg (K.) and Dössel (O.). – Cortex segmentation from 3D MR images for MEG reconstruction. *Biomagnetism: Fundamental Research and Clinical Applications*, 1995, pages 433–438.

BIBLIOGRAPHY

- [Wie93] Wieringa (H.J.). – *MEG, EEG and the Integration with Magnetic Resonance Images*. – PhD thesis, University of Twente, the Netherlands, 1993.
- [XPP⁺98] Xu (C.), Pham (D.), Prince (J.), Etemad (M.) and Yu (D.). – Reconstruction of the central layer of the human cerebral cortex from MR images. *Lecture Notes in Computer Sciences: Proceedings international conference on Medical Image Computing and Computer-Assisted Intervention*, vol. 1496, 1998, pages 481–488.
- [ZSSD98] Zeng (X.), Staib (L.), Schult (R.) and Duncan (J.). – Segmentation and measurement of the cortex from 3D MR images. *Lecture Notes in Computer Sciences: Proceedings international conference on Medical Image Computing and Computer-Assisted Intervention*, vol. 1496, 1998, pages 519–530.